ECMWF Newsletter

Number 155 – Spring 2018

European Centre for Medium-Range Weather Forecasts
Europäisches Zentrum für mittelfristige Wettervorhersage
Centre européen pour les prévisions météorologiques à moyen terme

www.ecmwf.int/en/about/news-centre/media-resources

CONTENTS

PUBLICATION POLICY

The *ECMWF Newsletter* is published quarterly. Its purpose is to make users of ECMWF products, collaborators with ECMWF and the wider meteorological community aware of new developments at ECMWF and the use that can be made of ECMWF products. Most articles are prepared by staff at ECMWF, but articles are also welcome from people working elsewhere, especially those from Member States and Co-operating States. The *ECMWF Newsletter* is not peer-reviewed.

Editor: Georg Lentze

Typesetting and Graphics: Anabel Bowen with the assistance of Simon Witter

Cover image: mishoo/istock/Thinkstock

Any queries about the content or distribution of the *ECMWF Newsletter* should be sent to Georg.Lentze@ecmwf.int

Guidance about submitting an article is available at www.ecmwf.int/en/about/news-centre/media-resources

CONTACTING ECMWF

Shinfield Park, Reading, Berkshire RG2 9AX, UK

Fax:		+44 118 986 9450
Telephone:	National	0118 949 9000
	International	+44 118 949 9000
ECMWF website:		www.ecmwf.int

Strategic advances

It has taken a lot of development and testing, but we are now in the last stages before implementing the latest upgrade of ECMWF's Integrated Forecasting System (IFS), scheduled to become operational on 5 June. There is an overall improvement in 2 m temperature in both high-resolution forecasts (HRES) and ensemble forecasts (ENS), particularly for Europe. Some negative impact is noted in upper air fields for the ensemble in the short range in the extratropics, but results are significantly positive across all ranges in the tropics. Changes in scores for the monthly system are generally positive across the range of parameters. Above all, this upgrade marks a milestone towards the delivery of our Strategy to 2025. A key element of the Strategy is the commitment to achieve coherence between our different forecasts, and this is now done. The coupling with the ocean, now extended to the HRES, substantially improves tropical cyclone intensity forecasts. It is making all our forecasts fully coupled and delivers a seamless approach between all ranges and forecasts.

But the advances brought by this upgrade do not stop there. A new lightning flash density scheme will provide additional guidance for severe weather prediction. This new product, presented in this Newsletter, will offer forecasts of average lightning activity with useful skill up to several days ahead. A full review of the upgrade will be included in the next issue of the Newsletter.

Our activities with the EU are continuing to flourish, with several projects successfully coming to fruition and delivering to expectations. These include ERA-CLIM2 and EarthServer-2. A few more projects relating to our Scalability Programme have just been approved. They include ESCAPE-2, MAESTRO and EPIGRAM-HS, which will allow us to continue the ground-breaking work that is under way to make our codes scalable.

This quarter has also provided us with an opportunity to showcase the work we do as part of the EU's Copernicus programme, at an event hosted by the European Parliament on 10 April. The event allowed us to highlight the synergies at the heart of the environmental sciences we cover, together with the progress achieved by the Copernicus Climate Change Service and the Copernicus Atmosphere Monitoring Service.

Finally, I wanted to touch on the Arctic Meteorological Summit hosted by Finland, which I attended and which was an opportunity to discuss the contributions that ECMWF is making to the Year of Polar Prediction. The Summit clearly highlighted the high level of collaboration already in place to enhance our Arctic monitoring capability, but also the urgent need to do more. Topics which were identified include the exchange of data and the need for a closer-knit working relationship between academia, meteorological services and polar experts. The APPLICATE workshop hosted at ECMWF in January 2019 will certainly give us more opportunities to discuss these topics.

Florence Rabier
Director-General

Predicting extreme snow in the Alps in January 2018

LINUS MAGNUSSON, DAVID RICHARDSON

January 2018 saw several episodes of extreme snowfall in the Alps, on both the northern and southern side of the mountain range. In this article we focus on the event that affected the south-western part from 7 to 9 January. Reports on the Web talked about 2 to 3 metres of fresh snow. The ski report for Tignes and Val d'Isère reported 110 to 160 cm of fresh snow in two days. Road links to several villages, such as Bonneval-sur-Arc in France and Zermatt in Switzerland, were cut by avalanches and tourists were stranded in the resorts.

The extreme precipitation in the south-western Alps was caused by a cut-off low centred over the western Mediterranean that stayed in a similar position for several days and brought moist air northward on its eastern side. The cut-off low was well predicted and ECMWF's Extreme Forecast Index (EFI) for total precipitation showed a signal more than a week in advance over the south-western Alps. The median of the ensemble forecast (ENS) starting on 1 January showed precipitation of 40 mm/48 hours in Val d'Isère for 7–8 January, and a risk of up to 100 mm. Between 2 and 3 January, the ensemble forecast became more extreme and the median jumped up to above 80 mm.

For all forecasts issued from 3 January onwards, the high-resolution forecast (HRES) gave higher two-day precipitation for 7–8 January in Val d'Isère than the ensemble median. This suggests a sensitivity to horizontal resolution (about 9 km for HRES and 18 km for ENS), which is expected in steep terrain. From the TIGGE-LAM archive hosted by ECMWF, we have access to eight different limited-area ensembles for evaluation purposes. Comparing the ECMWF global ensemble with the COSMO-LEPS ensemble with 7 km resolution from ARPA-ER SIMC in Italy, we find much higher precipitation accumulations in the limited-area ensemble. This is also true if we compare a short-range forecast from a random ensemble member from COSMO-LEPS with ECMWF HRES.

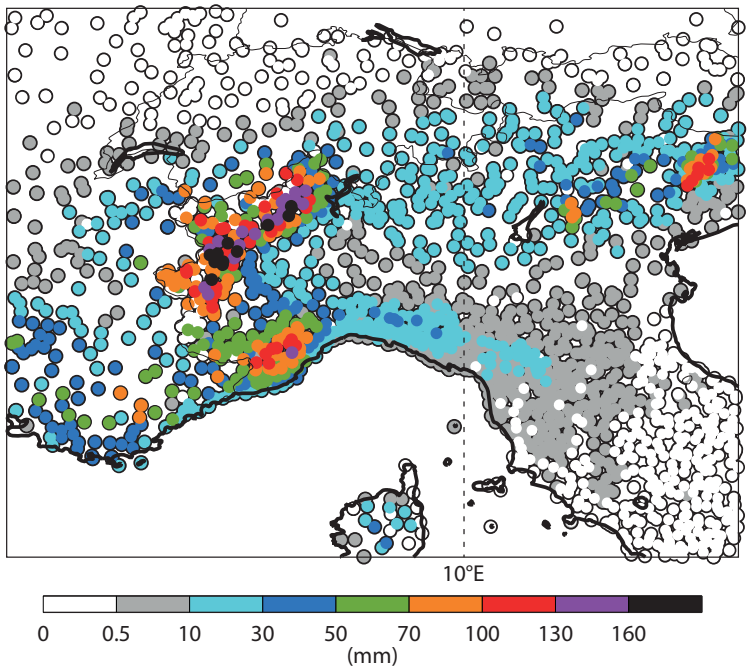

Observed precipitation. Twenty-four-hour precipitation between 8 January 06 UTC and 9 January 06 UTC, according to reports received from regional networks contributing to the high-density observation (HDOBS) project at ECMWF.

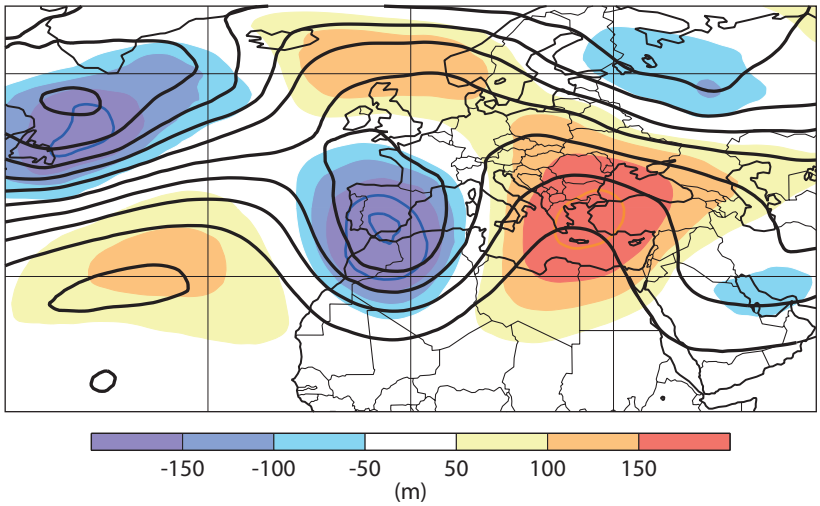

Cut-off low. The analysis of 500 hPa geopotential height (contours) and the corresponding anomaly (shading), averaged for 7–9 January, indicate the location of the cut-off low in the western Mediterranean that brought extreme precipitation to parts of the Alps.

Accurately predicting snow accumulation in complex terrain is difficult for current global models because of their relatively coarse grid spacing. It is impossible to resolve local differences in precipitation due to individual valleys and mountain peaks and local wind patterns. The lack of resolution for the orography also poses difficulties in predicting the freezing level relative to the terrain and whether the precipitation will fall as rain or snow. For verification, observing precipitation accumulation is very challenging during heavy snowfall. During fast accumulations of snow, rain gauge buckets can easily be filled by snow between being emptied, and automatic stations are known to have large errors during

intense snowfall. It is therefore very difficult to judge the performance of the forecasts in terms of total precipitation. What we can say is that the ECMWF forecast gave an early indication of unusually large amounts of precipitation in the Alps. However, with the lower amounts of about 40 cm for Val d'Isère in the earlier forecasts, there could have been an expectation that there would be nice skiing conditions with some fresh snow, while the outcome of probably three times as much or more resulted in closed pistes and tourists being trapped in the resorts.

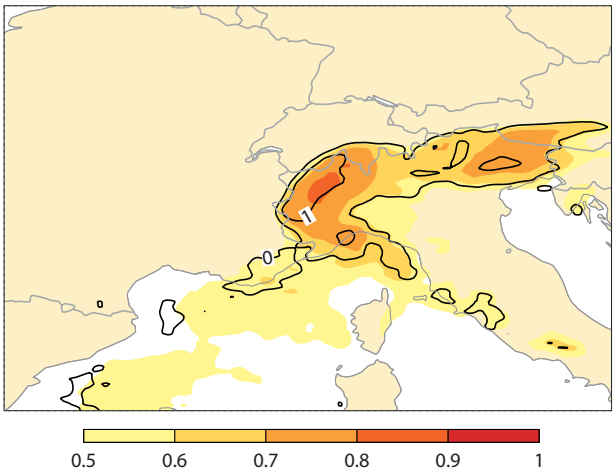

Extreme Forecast Index (EFI) and Shift of Tails (SOT). EFI (shading) and SOT (contours) for three-day total precipitation from 7 to 9 January in the forecast from 1 January.

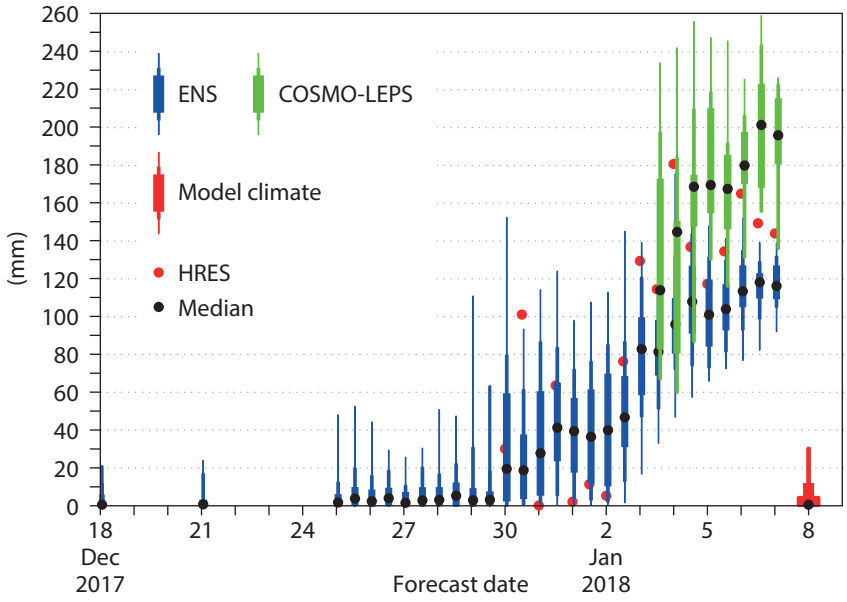

Ensemble forecasts for Val d'Isère. Total precipitation for Val d'Isère on 7 and 8 January as predicted by forecasts from different initial times. The box-and-whisker plots show the 1st, 10th, 25th, 75th, 90th and 99th percentile and the black dots show the median.

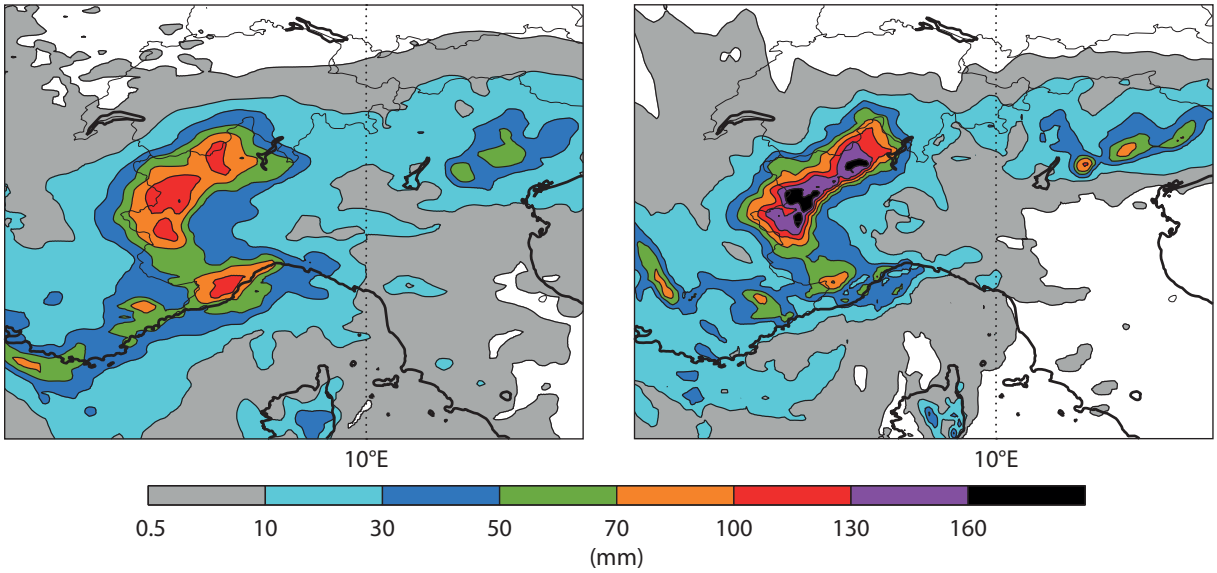

Short-range HRES and COSMO-LEPS forecasts. HRES precipitation forecast initialised on 8 January at 00 UTC for the period 8 January 06 UTC to 9 January 06 UTC (left) and the same forecast from a member of the COSMO-LEPS ensemble (right).

New study explains unusual 2015/16 El Niño heat budget

MICHAEL MAYER, MAGDALENA ALONSO BALMASEDA, LEOPOLD HAIMBERGER
(University of Vienna)

A new study uses ECMWF's ocean reanalysis ORAS5 to show that the unusual lack of cooling of the tropical Pacific upper ocean during the 2015/16 El Niño event can to a large extent be attributed to changes in heat transport from the Pacific into the Indian Ocean, which were in turn caused by changes in the Indian Ocean state.

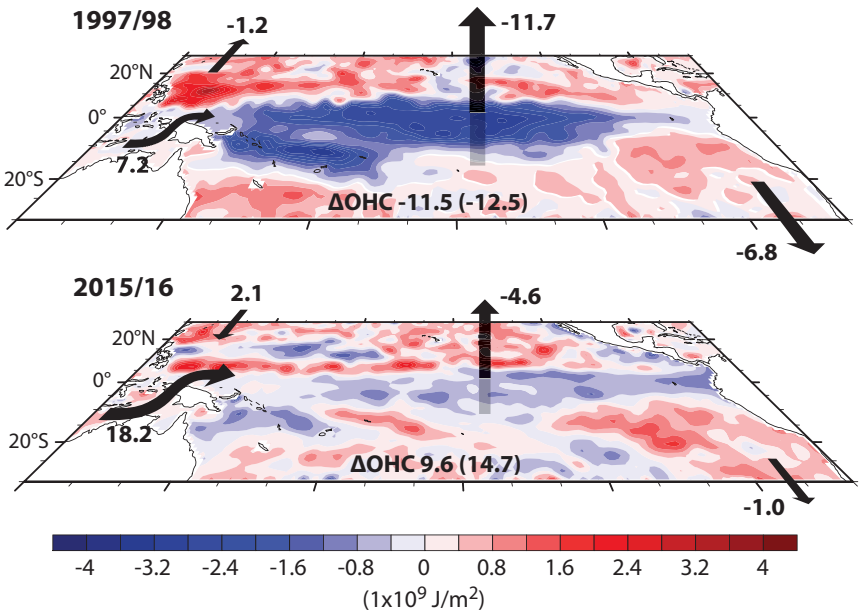

Upper ocean heat content changes. The changes are shown for the periods January 1997 to December 1998 and January 2015 to December 2016, based on ORAS5. Arrows and associated numbers (in zettajoules) indicate the direction and strength of two-year accumulated heat transport and flux anomalies across the boundaries of the tropical Pacific. For example, the positive numbers associated with the ITF represent reductions in westward ITF heat transports during the El Niño events. Integrated ocean heat content changes are given for 0–300 m and for the full-depth ocean (in brackets). Signs are chosen such that positive (negative) values indicate a contribution to a warming (cooling) of the Pacific.

An unusual El Niño

The 2015/16 El Niño was a strong event with peak sea-surface temperatures in the equatorial Pacific similar to those of the exceptional 1997/98 El Niño. Usually tropical Pacific Ocean heat content decreases during El Niño events, mainly due to enhanced evaporation associated with the anomalously warm sea-surface temperatures. This process usually leaves an anomalously cold tropical Pacific, which prepares the ground for a swing towards relatively cool La Niña conditions and the start of a new cycle.

A large fraction of the heat lost from the tropical Pacific Ocean during an El Niño event is transported out of the tropical Pacific region by the atmosphere, fuelling changes in weather patterns worldwide (teleconnections). The heat is eventually reabsorbed by the ocean in other regions of the world or radiated into space. Only a relatively small fraction of the exchanged heat is immediately lost to space via radiation in the tropical Pacific region. The net effect of typical El Niño events is thus to cool the tropical Pacific Ocean and the Earth system as a whole. For example, during the 1997/98 El Niño, the upper 300 m of the tropical Pacific (averaged between 30°S and 30°N) lost about 11.5 zettajoules (1 zettajoule = 10^{21} joules) to other parts of the Earth system, which is equivalent to about 20 years of world energy consumption.

However, the energetics of the 2015/16 event deviated substantially from this canonical behaviour. While there was sizeable cooling along the equator, the tropical Pacific upper ocean as a whole, instead of losing heat, gained about 9.6 zettajoules of heat during the 2015/16 El Niño. The absence of tropical Pacific cooling during the 2015/16 El Niño may explain why subsequent cool La Niña conditions were only weak and short-lived. Several unexpected weather extremes, such as the strong hurricane season in the Eastern Pacific during 2016 and the 'coastal El Niño' in 2017 that brought torrential rain to Peru and Colombia, can be attributed to the near-absence of La Niña conditions in 2016/17.

Use of ocean reanalysis

The study used various atmospheric and oceanic datasets to investigate the reasons for the differences between 2015/16 and 1997/98 in the coupled atmosphere–ocean energy budget. Satellite-based radiation data from CERES instruments and atmospheric reanalyses (e.g. ERA-Interim) were used for atmospheric diagnostics, while the oceanic part of the study strongly relies on ORAS5. Ocean reanalysis ingests various types of ocean observations (e.g. in-situ temperature/salinity profiles and satellite altimeter data) as well as boundary fluxes derived from atmospheric reanalysis into a dynamical ocean model to obtain a physically consistent estimate of the evolution of the ocean state. One particularly relevant output from ocean reanalysis is oceanic transports, which are relevant for regional oceanic heat budgets but difficult to measure directly.

Role of Indian Ocean state

An analysis of the heat budgets of the 2015/16 and 1997/98 El Niños reveals that differences in ocean heat export from the tropical Pacific can explain about 74% of the difference in the tropical Pacific Ocean heat content evolution between the two events. The main cause for this difference in oceanic heat export was the

different behaviour of the Indonesian Throughflow (ITF), which usually transports warm waters from the Pacific into the Indian Ocean. Heat transports associated with the ITF during 2015/16 were weaker than at any other time in the ORAS5 record (which begins in 1975). Further exploration shows that this weakening was linked to the relatively large warming and associated sea level rise in the Indian Ocean compared to other tropical ocean basins over the last decade, which has acted to decrease westward ITF volume and heat transports. The reduction of ITF heat transport in 2015/16 was strong enough to outweigh the surface heat loss of the tropical Pacific, leading to a net warming.

The results of the study point to the need for a realistic representation of Indo-Pacific energy transfers in ocean reanalyses and numerical models to further improve seasonal-to-decadal predictions. In particular, the correct initialisation of the sea level and associated temperature gradients between the Indo-Pacific basins plays a role in ENSO (El Niño–Southern Oscillation) predictions. Seasonal prediction experiments are currently under way at ECMWF to better characterise the impact of the Indian Ocean state on the evolution of El Niño events.

More details on the study can be found in an article published by the journal *Geophysical Research Letters* (doi:10.1002/2018GL077106).

TV weather presenters explain Copernicus data

SILKE ZOLLINGER

The Euronews channel has begun to give climate and air quality updates using data from the Copernicus Climate Change Service (C3S) and the Copernicus Atmosphere Monitoring Service (CAMS). Weather presenters for a number of national TV channels have also begun to incorporate C3S information into their reports. The development is part of a drive by the two EU-funded Copernicus services operated by ECMWF to broaden the audience for the climate and atmospheric composition information they provide.

Since December 2017, Euronews has been airing exclusive daily 24-hour air quality forecasts for Europe in 41 countries and monthly updates dedicated to the planet's changing climate in 156 countries. Based on CAMS data, an index ranging from 1 (very good) to 5 (very poor) is used to provide air quality forecasts for major European cities. The monthly climate update presents the latest C3S climate data for Europe and the world and explains how recent events relate to climate change.

Climate attribution

TV weather presenters in countries such as Belgium, Germany, Greece, the Netherlands and Switzerland have begun to explain Copernicus data to their audiences. Among other things, the data can help them to clarify the links between weather events and climate change. Özden Terli, a weather presenter at the German publicly-funded TV channel ZDF, says there is growing interest in understanding such links. "It's very important to speak regularly about climate change and how the already changed climate influences weather patterns," he recently told the Up Front magazine published by the International Association of Broadcast Meteorology (www.iabm.org/latest-up-front). He says that it is useful for people to know that certain weather events, such as the heatwave in southern Europe in the summer of 2017, are much more likely today than they were in pre-industrial times.

Copernicus data on TV. ZDF weather presenter Özden Terli uses a C3S chart to illustrate that 2017 was the warmest year on record not influenced by warming El Niño conditions, when compared to the period 1981 to 2010. *(Screenshot: ZDF, Özden Terli, ECMWF Copernicus Climate Change Service).*

Dick Dee, the Deputy Head of C3S, emphasises that any climate attribution must be scientifically sound. It can only be about probabilities as no individual weather event can be said to be caused by climate change. "The idea of attribution is to see whether the statistics of extreme weather events are affected by climate change," he says. Dick and his C3S colleagues are in the initial stages of setting up a pilot scheme that will be able to perform the necessary calculations within a week of specific weather events. To begin with, the scheme will look at cold snaps and heat waves since these are the kind of events for which the best statistics are currently available. The pilot scheme is due to be launched in 2019. In the meantime, weather presenters who wish to use C3S monthly climate charts and data in their broadcasts can obtain these from the C3S website: https://climate.copernicus.eu/monthly-maps-and-charts.

ERA-CLIM2 outcomes boost NWP and climate work

ROBERTO BUIZZA

ERA-CLIM2, a three-year European Union 7th Framework project that ended in December 2017, has made a major contribution to climate research and the development of climate monitoring services through its data rescue activities, post-processing of observations and work on coupled data assimilation methods. In particular, it has produced two coupled reanalyses, i.e. physically consistent datasets describing the evolution of the global atmosphere, ocean, land surface and cryosphere and the carbon cycle.

ECMWF played a key role in this collaborative project from the beginning: Dick Dee submitted the original proposal and acted as project coordinator until September 2015, when the author of this article took over. Magdalena Alonso Balmaseda, Manuel Fuentes and Patrick Laloyaux were work package leaders, and several other members of staff worked for the project on aspects of the science, technology, management and accounting.

The project has been at the heart of a concerted effort in Europe to build the information infrastructure needed to support climate monitoring, climate research and climate services, based on the best available science and observations. More specifically, ERA-CLIM2 was one of the designated precursor projects of the EU-funded Copernicus Climate Change Service (C3S). It was intended to help build the infrastructure and production capabilities of C3S, which is being implemented by ECMWF. ERA-CLIM2 has achieved this goal by making substantial contributions to reanalysis research in four main areas:

- **Observation data rescue and post-processing:** ERA-CLIM2 funded a major effort on data rescue for historical in situ weather observations around the world, and substantial work on the reprocessing of satellite climate data records to enable their use for reanalysis.
- **Data assimilation methods:** ERA-CLIM2 led to the development and testing of coupled data assimilation methods, capable of including observations from different Earth system components (land surface, ocean, sea ice, atmosphere, chemical components, etc.) in a consistent manner, to produce a more consistent estimate of the evolution of the Earth system, especially at the surface. This will help to develop coupled data assimilation in numerical weather prediction (NWP).
- **Reanalysis production:** ERA-CLIM2 generated innovative reanalysis datasets, such as the first European coupled ocean–land–atmosphere reanalysis of the 20th century (CERA-20C), which also includes the carbon cycle; a nine-year higher-resolution coupled reanalysis of the satellite era (CERA-SAT, see the separate article by Dinand Schepers in this Newsletter); and an ocean reanalysis of the 20th century, ORA-20C.
- **Evaluation and uncertainty estimation:** ERA-CLIM2 has advanced our understanding of the quality of uncoupled and coupled reanalyses, and it has led to the development of methods for estimating uncertainty in reanalyses.

Understanding climate change is highly dependent on the availability of global satellite and conventional observational data for the atmosphere, the land, the ocean and sea ice, and on the development of coupled ocean–land–atmosphere models and assimilation systems that can ingest these data. A continuous cycle of research and development activities in data assimilation, data rescue, observation reprocessing, production, and diagnosis and evaluation is required to improve future reanalyses, so that they can provide a continuously improving depiction of the evolution of the Earth system.

Ocean heat content

CERA-20C and CERA-SAT are ensembles of coupled reanalyses, the first of their kind, a fact that opens new opportunities but also poses new challenges for evaluation. The distribution of the ensemble members should be a realistic representation of the uncertainty associated with the reanalysis. To check this, one can for example compare the reanalysis against other reanalysis products or against independent observations. A comparison of the ocean heat content (OHC) of the upper 300 m in the CERA-20C ensemble and in dedicated ocean reanalyses shows good agreement overall. The large spread

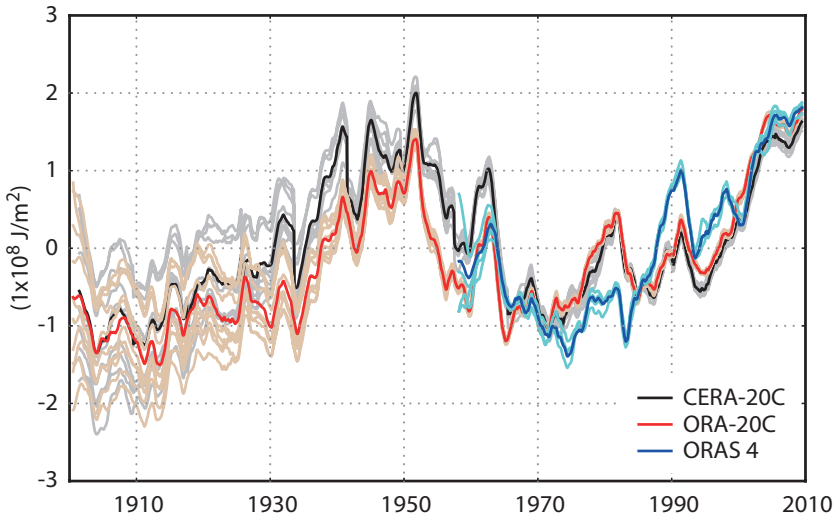

Global 0–300 m ocean heat content anomalies with respect to 1958–2010. The chart shows results for the ORA-20C ocean reanalysis ensemble (10 members), the CERA-20C ensemble (10 members) and the ORAS4 ocean reanalysis ensemble (5 members), with faint lines showing the ensemble members and bold lines the ensemble mean. An OHC increase of 1x10^8 J/m^2 corresponds to a temperature increase of 0.08 K averaged over the top 300 metres.

among the 10 members of the CERA-20C reanalysis before 1950 is consistent with the sparse observation coverage during that time. It provides a measure of the uncertainty in the reanalysed state of the ocean during those decades. Short-term variations at other times are caused by internal variability and/or volcanic eruptions, of e.g. Agung (1963), El Chichon (1982) and Pinatubo (1991). These eruptions all led to a temporary cooling of the upper ocean. The increase in OHC since 1970 is consistent with observations and is the manifestation of global warming in the ocean state.

CERA-20C also performs well in comparisons of different ensembles against independent observations. For example, a detailed evaluation of precipitation in CERA-20C and ERA-20C (the uncoupled reanalysis produced in the ERA-CLIM project that preceded ERA-CLIM2) with rain gauge-based precipitation estimates from GPCC (Global Precipitation Climatological Center) indicates overall better quality for CERA-20C, particularly in Africa and the Indian Monsoon region.

ERA-CLIM2 in numbers	
10	The number of ensemble members in the CERA-20C and CERA-SAT reanalyses.
110	The number of years covered by CERA-20C (from 1901 to 2010).
1,100	The approximate number of person-months funded by the European Union contribution to the ERA-CLIM2 project.
500,000	The approximate number of coupled data assimilation cycles needed to generate the 110-year CERA-20C reanalysis.
700,000	The approximate number of station-days of upper-air data that have been rescued and digitised as part of ERA-CLIM2.
1,300,000	The approximate number of snow-course observations that have been rescued and digitised as part of ERA-CLIM2.
2,200,000	The approximate number of station-days of surface data that have been rescued and digitised as part of ERA-CLIM2.
1,600 terabytes	The amount of CERA-20C data.

ERA-CLIM2 and C3S

The Copernicus Climate Change Service has been able to transfer the ERA-CLIM2-funded research and development into operational systems and services. It has also succeeded in integrating the outcomes of ERA-CLIM2 and the other four precursor projects – CLIPC (Climate information portal), EUCLEIA (European climate and weather events: interpretation and attribution), QA4ECV (Quality assurance for essential climate variables) and UERRA (Uncertainties in ensembles of regional reanalyses) – into user-oriented applications.

Examples of ERA-CLIM2 activities with a high potential for use in C3S are:

- Development of a coupled assimilation system (three-dimensional ocean, sea ice, land and atmosphere) that can be used to generate climate reanalyses for the 20th century and consistently derived reanalyses of the global carbon cycle; the version of the CERA (Coupled ECMWF ReAnalysis) system used to generate CERA-SAT has been handed over to C3S so that it can be used as a prototype coupled assimilation system to generate the next C3S reanalysis, ERA6.
- Development of a global data rescue registry to keep track of in situ climate data rescue efforts worldwide, based on activities started in ERA-CLIM and pursued in collaboration with the ACRE initiative and many other existing data rescue efforts and projects.
- Development of a global in situ snow data collection based on work started in the CORE-CLIMAX coordination activity.
- Further development of the ERA-CLIM Observation Feedback Archive and associated tools.

Numerous quality-controlled historical weather observations with potential high impact for climate reanalysis rescued and/or post-processed within ERA-CLIM2 have already been added to international public data collections such as ICOADS (International Comprehensive Ocean–Atmosphere Data Set) and ISPD (International Surface Pressure Databank), for use in reanalysis and other climate applications.

Website and data access

The ERA-CLIM2 project website (http://www.era-clim2.eu/) includes information about the project and all reports associated with the project's deliverables, links to data portals and links to relevant reanalysis websites. It also includes links to web pages on the four project General Assemblies, where all presentations can be accessed and downloaded.

ERA-CLIM2 reanalyses can be accessed from dedicated data portals, such as the MARS archive catalogue portal: http://apps.ecmwf.int/archive-catalogue/. Links to other sites where data can be accessed can be found on the ERA-CLIM2 website: http://www.era-clim2.eu/dataportals.

ERA-CLIM2 was funded under the European Union Grant Agreement No. 607029 under the title 'European Reanalysis of the Global Climate System'. Its successful conclusion has been made possible by the outstanding commitment and work put in by the partner organisations and individuals involved in the project.

The ERA-CLIM2 Consortium: ECMWF (co-ordinating organisation) • UK Met Office • EUMETSAT • Universität Bern, Switzerland • Universität Wien, Austria • FCiências.ID, Portugal • All-Russian Research Institute of Hydrometeorological Information – World Data Centre • Mercator Océan, France • Météo-France • DWD, Germany • CERFACS, France • CMCC, Italy • Finnish Meteorological Institute (FMI) • The University of Reading, UK • Inria, France • Université de Versailles Saint-Quentin-en-Yvelines, France

EarthServer-2 shows benefits of OGC web services

JULIA WAGEMANN, ANTONINO BONANNI, STEPHAN SIEMEN, VLAD MERTICARIU (rasdaman, Germany), **KOSTAS APOSTOLOPOULOS** (CITE, Greece)

ECMWF hosted the last project meeting of the EarthServer-2 project at the beginning of March. The three-year EU-funded Horizon 2020 project explored the use of standardised web services for efficient access to large data volumes. Two standard data-access protocols defined by the Open Geospatial Consortium (OGC), designed to offer web-based access to multi-dimensional geospatial datasets, were explored: (i) Web Coverage Service (WCS) and (ii) Web Coverage Processing Service (WCPS), which is an extension of WCS. The project has enabled ECMWF to better understand the needs of the wider user community and will help to build new, targeted services in the future.

OGC web services

ECMWF already delivers large amounts of forecast data in real time to its users and data from its MARS archive to the meteorological community. These services work well for users in the meteorological community, but businesses and scientists from non-meteorological domains wanting to integrate meteorological data into their services often struggle with domain-specific interfaces, data formats and data volumes. Web services offer easier and customised access to the data: data is accessed via the Internet using a URL and can thus easily be integrated into web or desktop applications and scientific workflows. One of the main advantages of web services is the possibility to retrieve time-series data. Especially users of climate data are interested in retrieving climate information for specific locations. Retrieving time-series information directly saves users from time-consuming downloads and extracting information from large amounts of data.

Web services using OGC standards bring several additional benefits. OGC standards provide data access in a standardised way which is already well established in the world of geospatial information systems (GIS). This makes it easier to exchange or combine data from different data systems. Instead of learning how to access data from different systems, users merely have to learn the structure of an OGC web service request. The same structure is applicable to any OGC web service. An added benefit of using standards is vendor neutrality. Service providers can choose from different solutions to provide a standard web service endpoint.

Data access on demand can easily be integrated into data processing workflows. Data does not have to be downloaded any more but can be accessed directly from the server hosted by the data provider. Data processing or analysis workflows with Jupyter notebooks, for example, can easily be shared and reproduced among team members and colleagues.

Challenges

The project revealed some challenges in offering web services operationally. Data provided by a web service should be described by relevant metadata, for example units of measure. The metadata is ideally taken directly from the source data. Furthermore, a web service should offer suitable data output formats. JSON-based formats are particularly useful for rapid web application development. Output based on a data request should also be accompanied by associated metadata, such as appropriate axis labelling. Some OGC standards allow users to request extensive processing of the data on the server. The management of such an option is quite challenging on an operational system if the system cannot estimate the resource requirements of each request. The project was a chance for ECMWF to explore this scenario.

For ECMWF it was important to investigate how such a service could be provided for the MARS archive. One of the main obstacles is to link an asynchronous data service (ECMWF's MARS archive) with a

Hackathon. EarthServer-2 participated in two hackathons held at ECMWF. These were great opportunities to interact with users.

Developing the MARS rasdaman connection

The ERA-Interim reanalysis was chosen to be the first on-the-fly dataset accessible through the MARS-rasdaman interface. Data is retrieved through a multi-step approach that completely abstracts the data retrieval from the MARS syntax. The approach achieves the efficient retrieval of data from MARS by using the rasdaman array-based database technology and FeMME, a metadata manager that hosts metadata to enable the two systems to communicate with each other. The steps can be summarised as follows:

1. The user sends a WCS request to the public-facing interface of the service and the request gets translated into a corresponding MARS request.
2. The MARS request then gets dispatched internally and placed in the queue.
3. The data retrieved from MARS is then registered into the rasdaman database (according to pre-defined and data-dependent configuration files that define how data is mapped).
4. Finally, a response to the user is sent as soon as the data is available for download. This way, the user is able to send queries for analysis-ready-data without fetching potentially large GRIB files and the necessity to write explicit requests to the MARS system. At the same time, this approach benefits from the extensive data-processing functionalities of the processing extension (WCPS) of the WCS standard.

Ideally, data retrieved from the archive is cached into the rasdaman database for a pre-determined amount of time. This guarantees that subsequent requests of the same dataset can quickly access the data already ingested in rasdaman without the need for a further (potentially time-consuming) new data retrieval from the archive. This mechanism is built on top of the already existing MARS caching logic and is expected to further improve the response time of a request. More advanced caching policies can be developed as soon as more statistical data about service usage is available.

The advantage of this architecture is twofold. Firstly, the user can interact with the service through plain WCS requests without retrieving (and then post-processing) large amounts of meteorological and climate data. Secondly, there is no need to ingest large amounts of potentially unused data into the rasdaman database. This makes the approach scalable and suitable for larger databases.

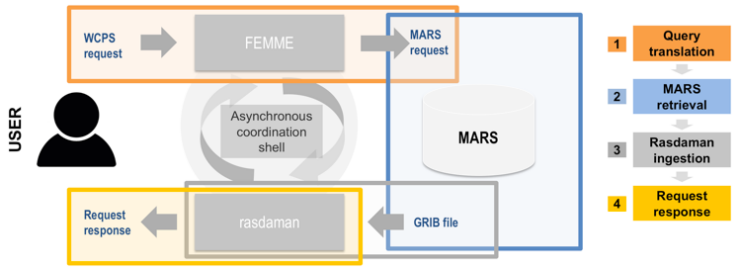

Workflow. Schematic representation of an OGC web service workflow for the MARS archive using FeMME and rasdaman.

synchronous on-demand service (OGC web services). To achieve this, the project tested combining MARS with the rasdaman (raster data manager) array engine, which is designed to work with massive multi-dimensional arrays such as those used in the Earth, space and life sciences (for details, see the box).

As part of the project, EarthServer also supported two hackathons hosted at ECMWF to engage with the user community. It was very useful to see how users were interacting with the OGC web services provided by the project.

While OGC web standards define the interface and interaction, many details of the implementation are left to the service provider. To ensure all services follow the same conventions on how data is accessed and offered, the community needs to agree on a profile. Such a profile for meteorological data offered by WCS (Web Coverage Service) 2.0 is under development with the Met Ocean Domain Working Group of the OGC.

Main project outcomes

The EarthServer-2 project has explored new ways to make ECMWF's varied and large datasets available to a wider user community. This is important for ECMWF's core operations as well as its activities relating to the EU-funded Copernicus Earth observation programme. ECMWF participates in the Met Ocean Domain Working Group and will aim to follow their guidelines, such as the MetOcean profile for WCS 2.0.

ECMWF would like to thank all those who tested the project's OGC Web Coverage Service (WCS) endpoint and provided valuable feedback on the test service during the project. This service will continue to run until June 2018. The lessons of the project will feed into new developments for web services at ECMWF.

More South American NMHS use ECMWF products

UMBERTO MODIGLIANI, EMMA PIDDUCK

Three more South American national meteorological and hydrological services (NMHS) have signed up for ECMWF web and data products in recent months. Following the emergency provision of real-time data during floods in Peru in March 2017 (see *ECMWF Newsletter* No. 152), ECMWF signed a new full NMHS non-commercial licence with the Peruvian Meteorological and Hydrological Service (SENAMHI). The one-year contract started on 28 December 2017. It gives access to both real-time data and web products (ecCharts). Also in December, a similar licence was signed with the Chilean weather service (Dirección Meteorológica de Chile). In February 2018, ECMWF also signed a new web NMHS non-commercial licence with Ecuador. The contract is for one year and gives Ecuador access to web products (ecCharts). The following South American countries have full NMHS non-commercial licences: Chile, Colombia, and Peru. In addition to these countries, Argentina and Ecuador have a web NMHS non-commercial licence.

The price for a full NMHS non-commercial licence is 42,000 euros per year while that for a web NMHS non-commercial licence is 3,500 euros per year. For more information on available licences, see the ECMWF licences web page: https://www.ecmwf.int/en/forecasts/accessing-forecasts/licences-available.

ECMWF briefs Ibero-American NMHS on Copernicus

EDUARDO PENABAD RAMOS

The 14th CIMHET meeting (Conference of the Directors of Ibero-American Meteorological and Hydrological Services) took place from 7 to 9 March in Willemstad, the capital of the Caribbean island of Curaçao. After the participation of ECMWF's Forecast Department in previous CIMHET meetings, on this occasion the organisers were keen to hear about the EU's Copernicus programme and the two services operated by ECMWF: the Copernicus Atmosphere Monitoring Service (CAMS) and the Copernicus Climate Change Service (C3S).

During the third working session of the meeting, entitled 'Provision of Weather, Climate and Hydrological Services', we presented the wealth of products and services already available from CAMS and explained the capabilities of C3S's Climate Data Store (CDS). As a taster of the latter, our presentation of the ERA5 reanalysis currently in production and of C3S multi-model seasonal forecast datasets attracted a lot of interest among the participants. Other topics discussed at the meeting included training, institutional development and resource allocation and the proposed restructuring of World Meteorological Organization governing bodies. The final Conference declaration explicitly took note of the interest in CAMS and C3S products and acknowledged ECMWF's attendance at the meeting.

CIMHET meeting participants. Delegates from 20 Ibero-American meteorological and hydrological services, the WMO, Regional Climate Centres and international organisations took part in the meeting.

CIMHET was established in 2003 to develop an Ibero-American Cooperation Programme in Meteorology and Hydrology bringing together the national meteorological and hydrological services (NMHS) of Spanish- and Portuguese-speaking countries in the Americas and the Iberian Peninsula. The Conference is coordinated by the Spanish meteorological service AEMET (Agencia Estatal de Meteorología) and is mainly funded by a trust fund started by the Spanish Government and its international development cooperation agency (AECID).

Member States value ECMWF visits, survey shows

ANNA GHELLI

A survey on a regular programme of liaison visits by ECMWF to its Member and Co-operating States shows that the visits are highly appreciated but that there is scope to improve their planning. The survey was sent out in December 2017, at the end of the 2015–2017 cycle of visits.

What did you say?

The words most often used by participants in the survey to describe the visits relate to networking, knowledge exchange and opportunities. This reflects the ethos on which the programme is based.

The inclusion of training is generally appreciated, and the creation of eLearning is felt to be a further improvement to ECMWF's training programme. Such online resources provide the basic knowledge needed to effectively use our products or software. They also support people in their learning journey towards more complex meteorological concepts.

Some respondents would like to have more time to plan the visits in their local organisation and country. Many stakeholders need to be contacted and coordinating this activity may be quite onerous. This year we will try to have a longer-term plan to support our local organisers.

Tailoring is another key aspect mentioned in the survey. In the last few years we have tried to collect information on possible topics of interest in advance of a visit. This does not always work, mainly because of a lack of time. Here too, longer-term planning of the visits may result in more input from the Member and Co-operating States. We are also aware that the number of ECMWF data users in each country has increased over the years, and that the spectrum of applications and consequently interests is becoming more diverse. The question of how best to tailor the visits may thus need revisiting: we need innovative ideas on how to engage with this wider community. This aspect will be reviewed in the course of this year with the Member States who have raised concerns.

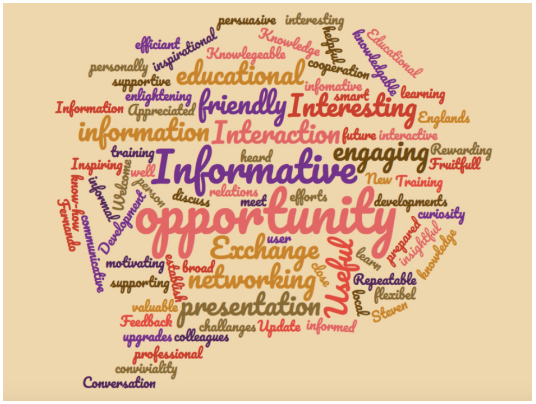

Word cloud. These are the words participants in the survey used to describe ECMWF's visits.

A long tradition

ECMWF has a long tradition of visiting its Member and Co-operating States. The main aim of the visits has always been the continuous provision of information about ECMWF to all interested staff at the respective national weather services. These events are an important opportunity to promote new ECMWF products. In the early 1990s, for instance, the visits were valuable occasions to present ECMWF's work on probabilistic forecasts.

Over the last ten years, the range of potential topics has increased as many Member and Co-operating States post-process ECMWF model output and develop applications that make use of ECMWF data. Opportunities to provide feedback to ECMWF about operational and research activities have also increased with the introduction of the Forecast User web page and a dedicated session at the annual user meeting. In these forums, ECMWF data users can voice any concerns they may have about model performance or request new products.

Today the visits regularly cover the way users process ECMWF data and products. They also include training activities and opportunities for networking to foster a deeper engagement between the Centre and its funding bodies. This two-way communication is essential for the progress of scientific work at ECMWF as well as product development. It provides ECMWF with invaluable feedback and opportunities to support the communities that ECMWF wants to serve.

In recent years, there has been an increasing effort to tailor such visits by introducing ad-hoc training and webinars (remote seminars) and where possible by supporting training events organised locally or regionally.

Thank you to local organisers

December 2017 marked the end of the 2015–2017 cycle of visit. The creation of such cycles became essential to guarantee that each country is visited at least once every three years.

The local organisers work with ECMWF, staff at their national meteorological and hydrological service and other users of ECMWF data to define a list of priority topics to be covered during the visit. Specific training on the use of products or software can also be organised at this stage. The invaluable work of the local organisers who take care of communication and advertising makes these visits a success. ECMWF would like to thank the local organisers for their work!

What next?

The new cycle of visits has started, with planning already under way for the first 10 to 11 visits. Over the course of the year we will incorporate your suggestions into our plans. Please continue to provide your feedback via the official channel (servicedesk@ecmwf.int).

User feedback helps shape ECMWF's data services

EMMA PIDDUCK, UMBERTO MODIGLIANI, FABIO VENUTI

ECMWF has seen a steady increase in the number of commercial, research and national meteorological and hydrological service (NMHS) data licences in the past three years, with a growing number of industries looking to use meteorological data in their services. A user survey conducted in the summer of 2017 is helping ECMWF to improve its services by increasing data volume limits and working on a new pricing tool.

The results of the survey identify use of ECMWF data in at least 26 different industries ranging from agriculture and forestry to aviation, shipping, and traffic management. The most widely serviced industries by commercial licence holders are the renewable energy, agriculture, and commodities trading industries. Indeed, ECMWF has observed a growing number of commercial companies undertaking research in renewable energy forecasting. ECMWF is also part of a collaborative research project with Envision Energy and the UK Met Office, which aims to improve wind power forecasting. Meanwhile, NMHS respondents said they use the data primarily in agriculture, aviation, and disaster management.

The high-resolution 10-day forecast (HRES) is a preferred dataset for 75% of participants in the survey overall and 90% of commercial participants. This is closely followed by the 15-day ensemble forecast (ENS), with 63% and 70% for all user responses and commercial customer responses, respectively.

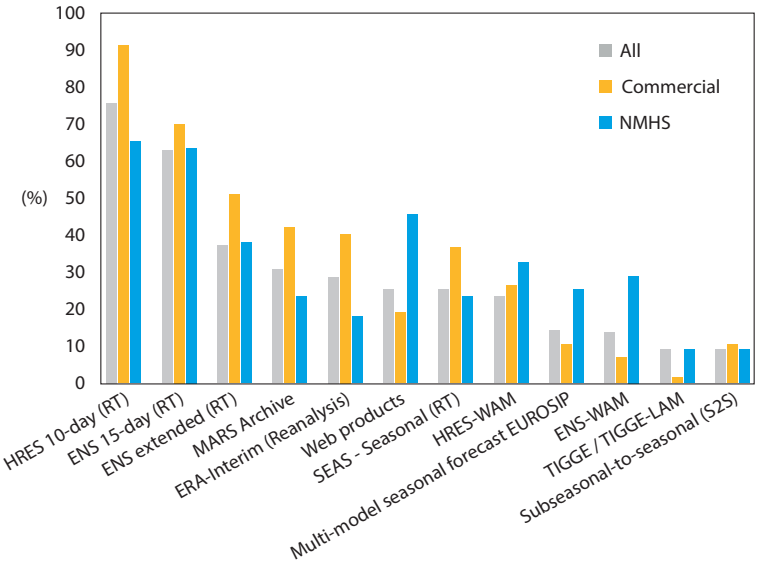

Preferred datasets. User survey respondents were asked to select preferred datasets from a set list. The chart shows the most popular ones. Real-time datasets are marked with RT.

When asked about their primary reason for using ECMWF data, most users (both commercial and NMHS) indicated that the quality of the data was the number one reason, followed by the reputability of the source. Many users commented on the length of time that they have been using ECMWF data: *"We have been using it for over a decade now because it is of good quality and from a reputable global producing centre."*

The survey sought to identify areas of improvement for the provision of ECMWF data, including services that users may wish to see in the future. One of the issues for commercial customers is the limit on the volume of data that is available with a licence. Additionally, users said that they would like to be able to generate their own quotes for data requirements using an online shopping application, the ability to access data at different height levels (meters above ground), and alternative data formats (e.g. netCDF). In response to these user requests, ECMWF has increased the volume cap, from 300 GB to 600 GB per day, and is developing a new pricing tool that will enable customers to generate their own prices. The tool will also streamline the licensing process for ECMWF and its Member States.

For more information on accessing ECMWF forecast data, please visit https://www.ecmwf.int/en/forecasts/accessing-forecasts.

ECMWF releases Atlas software library

WILLEM DECONINCK

ECMWF has publicly released Atlas, a software library supporting the development of Earth system model components and data processing, with an open source Apache 2 licence. The source code can be downloaded freely at www.github.com/ecmwf/atlas and contains installation instructions.

Emerging diverse and complex hardware solutions have a large impact on the programming models traditionally used in software for numerical weather prediction (NWP). Furthermore, NWP models are becoming increasingly complex as more Earth system components are introduced. Each model component may use different numerical algorithms and may be based on structured or unstructured grids.

In response, ECMWF is developing Atlas, an object-oriented (OO) programming library for developing flexible next-generation NWP models on existing and emerging hardware, such as GPUs. Atlas addresses the complexities associated with managing parallel

distributed data structures on Earth grids. It provides mesh-generation capabilities from a wide catalogue of grids. Through its OO design, the memory layout and parallelisation of fields defined on meshes can be abstracted to accommodate specific numerical methods and hardware implementations. Atlas not only supports structured global grids such as the ones used operationally at ECMWF, but also unstructured meshes and structured regional grids as used in limited-area models. Although Atlas's main features are implemented using C++, a modern OO Fortran interface allows Atlas features to be used in most existing NWP software packages.

At ECMWF, Atlas is being used in the development of a finite-volume module (FVM) for the Integrated Forecasting System (IFS) (see *ECMWF Newsletter* No. 145, pp. 24–29). Its parallel mesh-generation capabilities build a distributed unstructured mesh about the grid points of the IFS's reduced Gaussian grid. The resulting triangular or quadrilateral elements are then used to evaluate finite-volume differential operators. Atlas's mesh generator is also used in ECMWF's new Meteorological Interpolation and Regridding (MIR) software (see *ECMWF Newsletter* No. 152, pp. 36–39), where the resulting elements are used to construct linear interpolation operators.

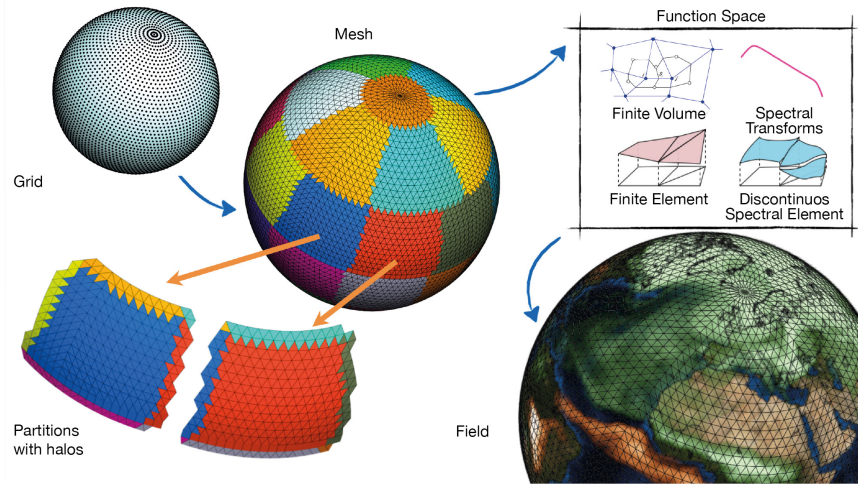

Distributed mesh generation. Atlas is here used to generate a distributed mesh from a very coarse reduced octahedral Gaussian grid. Each distributed mesh partition can be constructed with parallel halos to allow stencil operations. Distributed fields can then be created based on a specific 'function space', which is tightly coupled to numerical schemes of how discrete data is interpreted in a continuous space.

Atlas will be crucial in longer-term IFS developments. For example, in the EU-funded Horizon 2020 ESCAPE project it serves as a collaborative framework to develop next-generation building blocks, dubbed NWP and climate 'dwarfs', for NWP and climate models. In ESCAPE, these dwarfs are studied in isolation, optimised and ported to alternative hardware solutions, such as Intel's Xeon Phi and NVIDIA's GPU. Atlas's data structures and parallelisation routines therefore support synchronisation between CPU and GPU memory spaces.

New interpolation package MIR ready for testing

The new ECMWF interpolation package MIR (see *ECMWF Newsletter* No. 152) is now ready for testing by users of the MARS archive.

A version of the MARS client using MIR (MARS/MIR) is available on all ECMWF platforms and can be accessed using the command 'mars -m'. It can also be tested using the ECMWF Web API adding the key word 'ppengine=mir'. MARS/MIR is not considered ready for production at this point and should only be used for testing purposes.

MARS users are encouraged to test this new MARS/MIR client with their usual workload and report any problems or feedback to ECMWF.

The expected timeline for the operational implementation of MARS/MIR is as follows:

- June 2018: Release of a MARS/MIR client considered ready for production. The old MARS/EMOSLIB client will still be the default.
- Autumn 2018: MARS/MIR becomes the default version at ECMWF. The old MARS/EMOSLIB will still be accessible, but there will be no further updates to it.

Users can find more information about MARS/MIR in the ECMWF User Documentation wiki space, including the main differences and known issues:

https://software.ecmwf.int/wiki/display/UDOC/MARS+interpolation+with+MIR

This page will be updated to reflect any changes or new features, including the exact implementation dates. You may want to 'watch' this page to be notified about those updates.

doi:10.21957/plz731tyg2

Promising results for lightning predictions

PHILIPPE LOPEZ

Lightning is one of the most spectacular phenomena in the atmosphere. It can affect the environment by triggering wildfires. It can also disrupt air traffic and airport activities such as refuelling; cause power supply outages or power surges that can harm electronic equipment; damage buildings; and even lead to fatalities. Lightning also plays a significant role in the production of mid-tropospheric nitrogen oxides, which in turn influence the ozone budget.

Lightning is usually associated with intense convective activity and most commonly occurs in the troposphere. Somewhat fainter electrical luminous events that extend well above the top of convective clouds into the stratosphere and beyond, such as sprites, elves and blue jets, have started to be documented in recent years but their impact on human activities is negligible. Occasionally lightning can also be triggered in the ash cloud of volcanic eruptions. However, the focus of this article is on lightning produced by convection inside the troposphere, which is by far the most common cause.

ECMWF has developed a lightning parametrization that is expected to provide global predictions of lightning activity operationally from mid-2018. Experiments have shown that ECMWF ensemble forecasts (ENS) for lightning can have useful skill to at least day 3, while a good agreement with observations can be achieved in deterministic forecasts on temporal and spatial scales above 6 hours and 50 km.

Work is under way to enable the model to distinguish between cloud-to-ground and intra-cloud lightning. The possibility of assimilating observations from lightning imagers on new geostationary satellites is also being investigated.

Physics of lightning

From a physical point of view, convective lightning discharges occur in response to a local build-up of an atmospheric electric field. This field in turn results from the separation of positive and negative electric charges inside neighbouring convective regions. A highly simplified schematic of the typical tripole structure of electric charges inside a deep convective cloud is shown in Figure 1. A predominantly negatively charged layer is found between roughly –25°C and –10°C, below a deep positively charged layer extending toward the top of the cloud, and above another positively charged but shallower layer extending between the –10°C level and the base of the cloud. A more detailed description of the electrification mechanism inside convective clouds is given in Box A.

As illustrated in Figure 1, lightning flashes can be categorised as cloud-to-ground (when the electric discharge takes place between the cloud and the Earth's surface) or intra-cloud (when the discharge occurs between two cloud regions containing oppositely charged hydrometeors). These two types of lightning flashes will hereafter be referred to as CG and IC, respectively. The fraction of IC flashes is around 80% on average, although this percentage can fluctuate between 30% and 100% according to geographical location and thunderstorm characteristics. It is also worth noting that CG flashes are often characterised by much stronger peak currents (i.e. higher energy) than IC flashes.

Lightning observations

Continuous observations of lightning with wide spatial coverage are currently available from two main sources. First, several global, continental or national-scale networks of ground-based lightning sensors provide continuous monitoring of the location and, in some cases, of the intensity of lightning activity. The sensors work by detecting the electromagnetic emissions (so-called 'sferics') produced by individual lightning strokes. Most networks analyse sferics at either very low frequency (VLF; 3–30 kHz) or low frequency

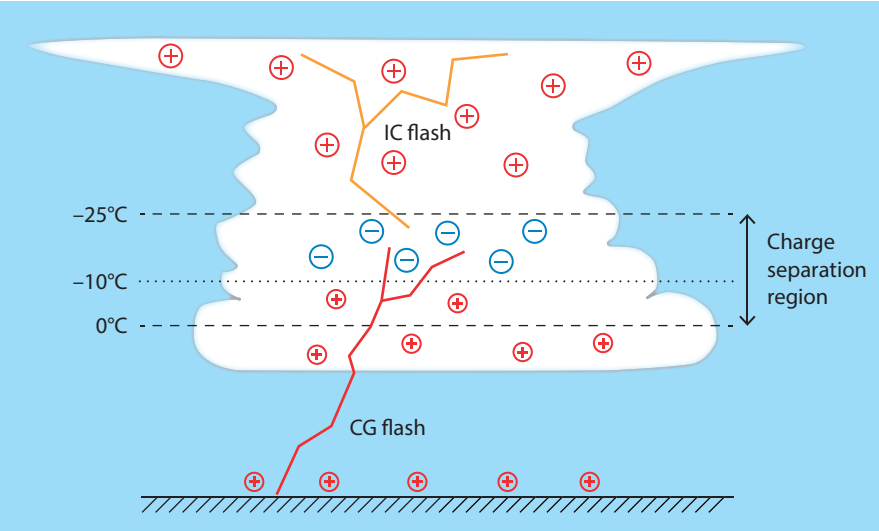

Figure 1 Simplified diagram of the typical distribution of positive (+) and negative (–) electric charges inside a thunderstorm cloud, with associated intra-cloud (IC) and cloud-to-ground (CG) lightning flashes.

How lightning is generated

A

The typical electric charge distribution shown in Figure 1 is the result of charge separation. Charges are separated during collisions between various types of hydrometeors with very different fall speeds, especially graupel or hail particles on the one hand and lighter ice particles or liquid water droplets on the other. Depending on whether the ambient temperature is higher or lower than about –10°C, graupel/hail particles involved in such collisions become positively or negatively charged, respectively. Both non-inductive and inductive processes are thought to be responsible for charge separation. By their nature, inductive processes require the existence of a sufficiently strong electric field in the environment and can thus only become effective after a preliminary electrification due to non-inductive processes. Once the electric field produced by charge separation locally exceeds a certain threshold, a lightning discharge can be triggered, which cancels out some of the charges. This in turn reduces the ambient electric field. A typical lightning discharge involves the preliminary ionisation of a channel that jerkily propagates through the atmosphere (a so-called leader), which can take several hundred milliseconds. Once the leader attaches to either the ground or another, oppositely charged part of the cloud, one or several strokes propagate through the ionised channel for a few microseconds each, producing very intense electric currents (typically 10 to 100 kA) and extremely high temperatures (typically 10,000 to 30,000 K). These successive strokes are the components of what one visually identifies as a lightning flash. The total duration of a flash usually remains well below a second.

(LF; 30–300 kHz), which allows their detection over a range of several hundred kilometres. Some of them can also operate at high frequency (HF; 3–30 MHz) or very high frequency (VHF; 30–300 MHz), although at such wavelengths the detection range is usually reduced. Using a method based on time of arrival (TOA) or magnetic direction finding (MDF) or both, the information from several sensors must be combined to locate individual lightning strokes with useful accuracy (a few kilometres or less). An additional estimate of the peak current of each stroke can also be obtained. Table 1 gives a non-exhaustive list of the largest networks currently in use and their characteristics, with a particular focus on Europe.

A major limitation of ground-based sensors is that their detection efficiency is often much lower for IC than for CG lightning strokes, due to the lower energy usually released by the former. Furthermore, detection efficiency and stroke location accuracy depend on the number of lightning sensors covering any particular area.

The other main source of lightning observations is space-borne imagers, which can detect the optical signature of lightning events at a wavelength of 777.4 nm (oxygen emission line). The identification of lightning pulses requires the continuous monitoring of the background scene and the detection efficiency is higher at night than during the day, when the background is brighter. Unlike ground-based sensors, satellite lightning imagers can identify both CG and IC lightning strokes with equal efficiency. The Optical Transient Detector (OTD; 1995–2000) and the Lightning Imaging Sensor (LIS; 1998–2013) were the first lightning imagers and were installed on board low-Earth-orbit (LEO) satellites. In 2017, a spare LIS instrument was installed on the International Space Station (ISS) for at least two years. More importantly, the new generation of geostationary satellites GOES-16 and GOES-17 (USA) and FY-4A (China) have all been equipped with lightning imagers (GLM and LMI, respectively). European Meteosat Third Generation geostationary satellites will have a similar lightning imaging capability (MTG-LI; from 2021). Once operational, and in contrast with previous LEO instruments, these new geostationary imagers will provide unprecedented observational coverage in both time (20-second refresh rate) and space (full Earth disc) at a resolution of around 8 km, with a flash detection efficiency greater than 70% and a location error better than 5 km.

Climatology of lightning

A widely used global climatology of lightning activity at 0.5° resolution was produced by *Cecil et al.* (2014) by combining satellite lightning imager observations from the OTD instrument (1995–2000) and the LIS instrument (1998–2010).

Network	Operator	Domain	Frequency	Detection type
ATDnet	Met Office	Europe, Africa	VLF	TOA
ENTLN	Earth Networks	USA, Brazil, Europe, Australia	VLF to HF	TOA
EUCLID	European consortium	Europe	LF	TOA + MDF
GLD360	Vaisala	Global	VLF	TOA + MDF
LDS	UBIMET	Europe, USA, Australia	VLF + LF	TOA
NLDN	Vaisala	USA	VLF + LF	TOA + MDF
WWLLN	University of Washington	Global	VLF	TOA
ZEUS	National Observatory of Athens	Europe	VLF	TOA

Table 1 List of wide-scale networks of ground-based lightning sensors and their main characteristics. **VLF** = very low frequency, **LF** = low frequency, **HF** = high frequency, **TOA** = time of arrival, **MDF** = magnetic direction finding.

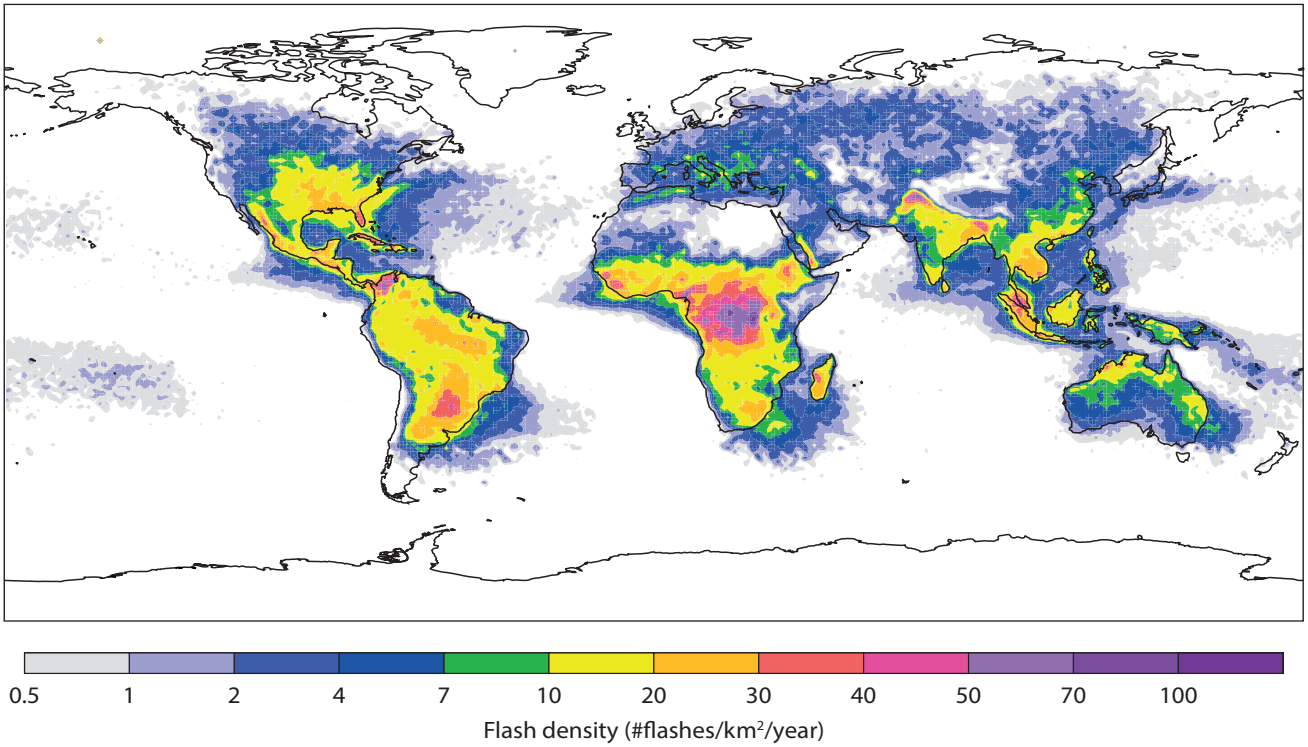

Figure 2 Annual mean flash densities from the LIS/OTD satellite climatology.

Figure 2 shows annual mean lightning flash densities from the LIS/OTD climatology. The overall mean lightning flash density of 2.86 per km^2 per year means that an average of 46.2 flashes are observed every second around the globe. Figure 2 highlights the world's major lightning hotspots: the Congo Basin (in excess of 50 flashes/km^2/year over a large area and locally in excess of 150), Colombia, Malaysia, the region south of the Himalayas and Florida. It also clearly shows the predominance of lightning over land in the overall mean. Possible explanations proposed for the much weaker lightning activity over oceans include the weaker convective updraughts and/or the lower aerosol concentrations in the marine planetary boundary layer (hence larger liquid droplets, heavier warm-phase precipitation and less graupel and hail available for charge separation). Of course, strong variations in lightning activity can be observed on the seasonal timescale (not shown), especially over extratropical land regions.

Parametrization of lightning in the IFS

A parametrization of lightning has been developed for ECMWF's Integrated Forecasting system (IFS) with two main purposes in mind: predicting lightning, i.e. the diagnosis of lightning activity for forecasting applications, and the assimilation of lightning observations, which might bring an improvement in the quality of ECMWF's atmospheric analyses and forecasts.

The parametrization estimates total (i.e. CG+IC) lightning flash densities using information about convective hydrometeor amounts, convective available potential energy (CAPE) and convective cloud base height, which are already diagnosed by ECMWF's convection scheme.

Lightning parametrization

B

In the version planned for operational implementation in IFS Cycle 45r1, the lightning parametrization does not discriminate between CG and IC flashes. It calculates total (i.e. CG+IC) flash density f_T (in flashes/km^2/day) as

$$f_T = \alpha\, Q_R \sqrt{CAPE}\, [\min(z_{base}, 1.8)]^2 \qquad (1)$$

where α is a tunable coefficient, currently set to 37.5 to match the annual global mean flash rate from the LIS/OTD climatology. The variable z_{base} is the convective cloud base height (in km). The term Q_R denotes a proxy for the charging rate resulting from the collisions between graupel particles and other types of hydrometeors inside the charging layer and is computed as

$$Q_R = \int_{z(0°C)}^{z(-25°C)} q_{graup}\,(q_{cond} + q_{snow})\rho(z)\,dz \qquad (2)$$

In Equation (2), q_{cond}, q_{graup} and q_{snow} denote the amount of convective cloud condensate, graupel and snow, respectively (in kg/kg), while $\rho(z)$ is the ambient air density (in kg/m^3) at altitude z. The amount of graupel and snow at each model level is diagnosed from the convective frozen precipitation flux P_f by writing

$$q_{graup} = \beta\, \frac{P_f}{\rho V_{graup}} \qquad (3)$$

$$q_{snow} = (1-\beta)\, \frac{P_f}{\rho V_{snow}} \qquad (4)$$

where β is set to 0.7 over land and 0.45 over sea, while constant fall speeds V_{graup} and V_{snow} for graupel and snow are assumed to be 3.0 and 0.5 m/s, respectively.

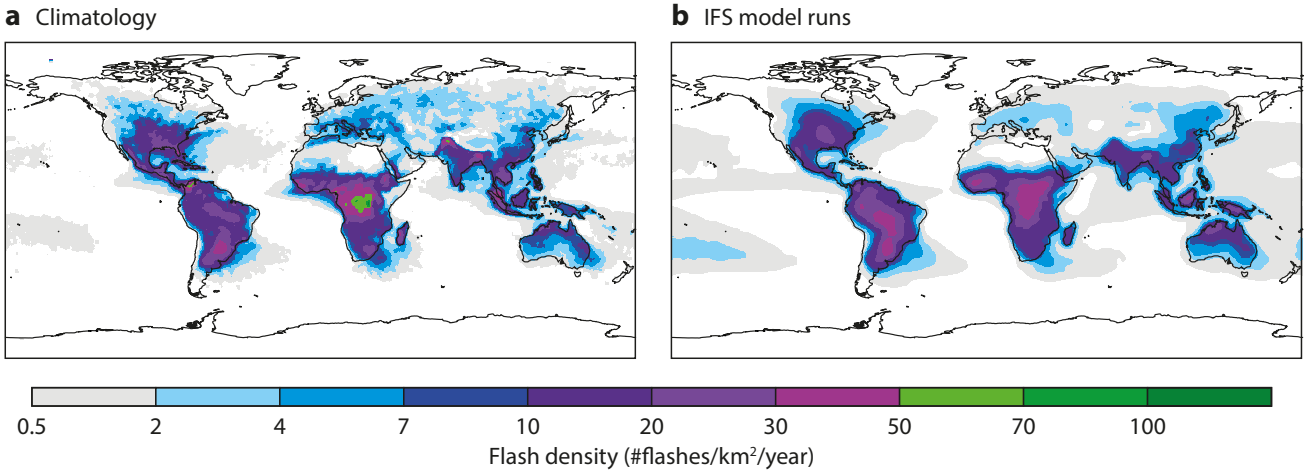

Figure 3 Annual mean lightning flash densities from (a) the LIS/OTD satellite climatology and (b) ten one-year-long IFS model runs, both at 80 km resolution. Note that panel (a) shows the same field as Figure 2, but at a coarser resolution.

More details on its formulation can be found in Box B as well as in *Lopez* (2016). The scheme has been calibrated to match the annual mean flash densities from the LIS/OTD satellite climatology of *Cecil et al.* (2014) shown in Figure 2. A linearised version of the lightning parametrization has also been coded and tested, since this will be an essential ingredient of the future 4D-Var assimilation of lightning observations.

From IFS Cycle 45r1, forecasts of both instantaneous and time-averaged total lightning flash densities will be available to ECMWF users.

Validation of the lightning parametrization

Figure 3 compares the annual mean total lightning flash densities computed from a series of ten 1-year-long IFS model runs at 80 km resolution with the LIS/OTD climatology. Overall, the spatial distribution of lightning activity from the model agrees well with observations. This is also true of its intensity, with the exception of the Congo Basin, where the extremely high climatological values are clearly underestimated in the model.

As an example of the performance at higher spatial resolution, Figure 4 compares time series of daily mean lightning flash densities over Europe from IFS deterministic short-range (0–24 h) forecasts at 18 km resolution with ground-based observations from UBIMET LDS (see Table 1) during the summer of 2015. On the continental scale, the day-to-day variations of model lightning agree quite well with those of UBIMET observations. The results are expected to be at least as good for the current highest operational resolution of 9 km. Naturally, this level of agreement is expected to degrade for smaller averaging times and areas. This is illustrated in Figure 5, which shows how the mean correlation between maps of IFS and UBIMET lightning flash densities varies with the averaging scale in both time (from 1 h to 24 h) and space (from 0.15° to 5°). Figure 5 suggests that accurately forecasting lightning on a scale of a few tens of kilometres and within an hour is still very challenging with the IFS. However, this is also true of other aspects of convective activity, such as precipitation (not shown). Model versus UBIMET lightning correlations do increase noticeably as the time and space constraints are relaxed (up to 0.75 correlation for daily averages over 5° boxes). Similar results are found against other observing networks (not shown).

In addition, the mean diurnal cycle of lightning activity in deterministic forecasts can be validated against ground-based lightning observations. To overcome the variable detection efficiency of ground-based networks, the observed and modelled lightning diurnal cycles are both normalised between 0 and 1, so as to focus on the lightning activity timing. As an example, Figure 6 shows mean diurnal cycle plots from the IFS and from three European ground-based networks of lightning sensors (ATDnet, EUCLID and UBIMET LDS) over the summer of 2015. The figure indicates that the simulated lightning

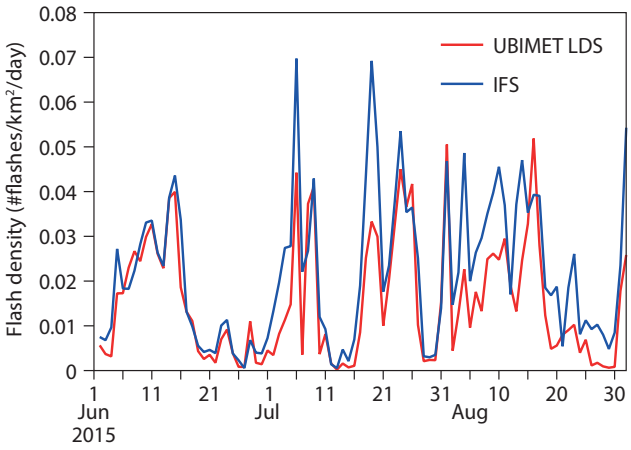

Figure 4 Time series of daily mean lightning flash densities from IFS short-range forecasts at 18 km resolution and from UBIMET LDS ground-based observations over Europe during the summer of 2015.

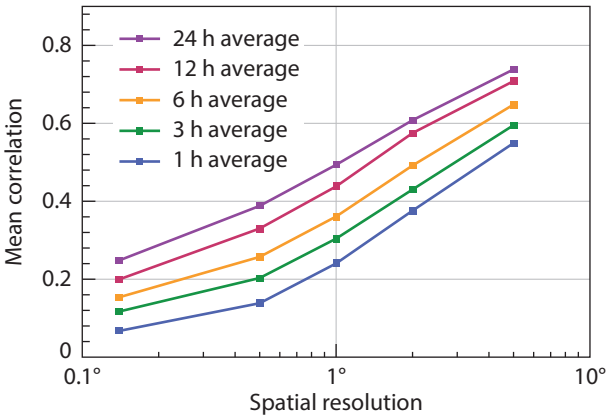

Figure 5 Mean map-to-map correlation for lightning flash densities between IFS short-range forecasts and ground-based observations from UBIMET LDS for different averaging periods as a function of averaging spatial resolution over Europe during the summer of 2015.

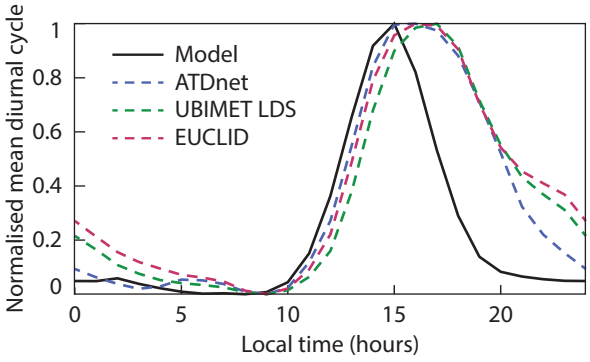

Figure 6 Mean diurnal cycle of lightning activity (normalised between 0 and 1) from IFS short-range forecasts at 18 km resolution and from three European ground-based networks of lightning sensors (ATDnet, EUCLID and UBIMET LDS) over the summer of 2015.

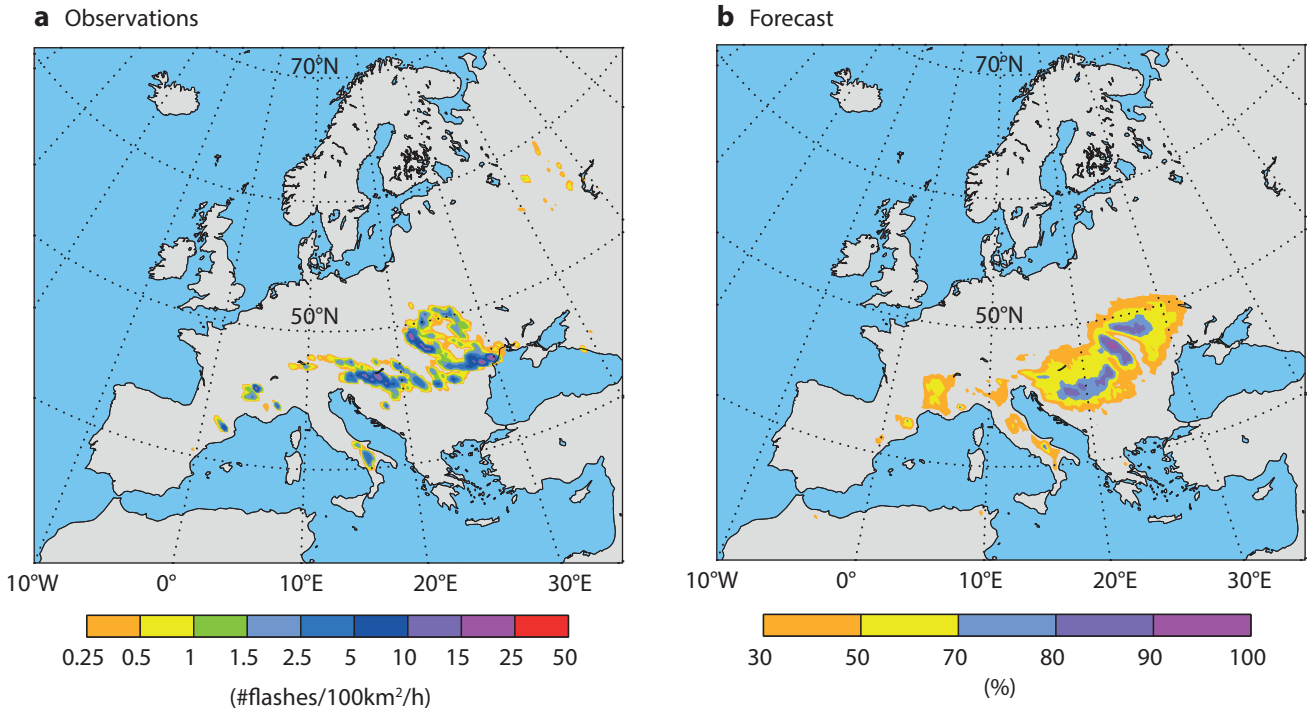

Figure 7 The charts show (a) ATDnet observed 6-hour mean lightning flash densities on 23 June 2017 at 1800 UTC and (b) the corresponding chart of the probability (above 30%) of lightning flash density exceeding 0.5 flashes/100 km^2/hour. Probabilities are based on a 51-member 66-hour ensemble forecast at 18 km resolution.

activity peaks at around 1500 UTC, which is about an hour ahead of the observed peak of activity. Furthermore and more importantly, lightning in the model tends to decay rather rapidly in the late afternoon, while observed lightning remains active until the middle of the night. This behaviour of simulated lightning is consistent with previous diagnostics based on the comparison of precipitation forecasts with ground-based radar observations. Past development efforts have brought the triggering of convection in the IFS into line with observations. However, simulated convective activity still vanishes too soon.

Finally, the discrete and random nature of lightning makes it particularly suitable for the probabilistic predictions provided by ensemble forecasts. For instance, using all the members of an ensemble forecast, it is possible to construct maps of the probability that lightning flash density will exceed a certain threshold. As an illustration, Figure 7 shows an example of such a probability map applying a minimum threshold of 0.5 flashes/100 km^2/hour to a 66-hour

ensemble forecast with 51 members. Figure 7 also shows ATDnet lightning observations to validate the geographical distribution of the simulated lightning. Even after almost three days of simulation, the ensemble approach is able to provide useful guidance on the regions expected to be affected by lightning, namely eastern Europe and to a lesser extent French and Italian mountain ranges, in this case.

Future developments

In parallel to the work on total lightning parametrization, efforts are under way to enable the model to discriminate between the CG and IC components of lightning. This would facilitate the quantitative evaluation of the model against ground-based networks of lightning sensors, which only provide a partial detection of IC flashes. Additional improvements of the current CG+IC lightning parametrization could come from revising its formulation as well as from future improvements of the IFS convective parametrization, upon which it depends. In order to maximise the usefulness of lightning scheme outputs to forecasters, the scheme will have to be evaluated more extensively, particularly in the context of ensemble prediction. The inclusion of lightning information in ECMWF's Extreme Forecast Index (EFI) might also be beneficial for severe weather prediction applications.

Work has also begun to explore the possibility of assimilating observations from the lightning imagers on board new geostationary satellites (GOES-16/GLM and possibly FY-4A/LMI, both recently launched, and MTG-LI from 2021). Of course, the successful assimilation of this type of observation will be very challenging. It will require finding the best compromise between the non-linear and discrete nature of lightning on the one hand and the requirements of linearity and smoothness that underpin the 4D-Var data assimilation method on the other. The hope is that lightning assimilation in ECMWF's 4D-Var system will eventually improve analyses and forecasts, particularly in the tropics during the rainy season and in extratropical regions in the warm season.

Finally, the performance of the lightning parametrization is also being tested in the IFS chemistry schemes for the simulation of nitrogen oxide emissions, with a potential improvement of the global ozone forecasts for the Copernicus Atmosphere Monitoring Service (CAMS) operated by ECMWF.

The work on the lightning parametrization described in this article has been greatly facilitated by the data from ground-based lightning detection networks kindly provided by UBIMET (Lightning Detection System; LDS), the European Cooperation for Lightning Detection (EUCLID), and the UK Met Office (Arrival Time Difference network; ATDnet). NASA's Global Hydrology Resource Center (USA) is also acknowledged for granting access to the LIS/OTD lightning climatology (*Cecil et al.* 2014).

FURTHER READING

Cecil, **D. J.**, **D. E. Buechler** & **R. J. Blakeslee**, 2014: Gridded lightning climatology from TRMM-LIS and OTD: Dataset description. *Atmos. Res.*, **135–136**, 401–414.

Lopez, **P.**, 2016: A Lightning Parameterization for the ECMWF Integrated Forecasting System. *Mon. Wea. Rev.*, **144**, 3057–3075.

doi:10.21957/cf724bi05s

Improved use of atmospheric in situ data

BRUCE INGLEBY, LARS ISAKSEN, TOMAS KRAL, THOMAS HAIDEN, MOHAMED DAHOUI

Atmospheric in situ observations from surface stations, aircraft and radiosondes are important both for direct use in the ECMWF data assimilation system and for diagnostics. Radiosonde and surface observations also help to control biases in the assimilation system. However, like other Earth system data, in situ observations can be complex to interpret and close attention to quality control, observation uncertainty and in some cases bias correction is needed to optimise their use.

This article describes a range of recent improvements in the use of atmospheric in situ observations at ECMWF. One of these has been made possible by the gradual transition in reporting such observations from alphanumeric codes (such as TEMP and SYNOP) to Binary Universal Format for the Representation of meteorological data (BUFR): extra information in BUFR enables balloon drift to be taken into account in the assimilation of radiosonde data. A change to this effect will be implemented in the next upgrade of ECMWF's Integrated Forecasting System (IFS Cycle 45r1).

Other improvements in the next IFS upgrade include better bias correction and reduced thinning of aircraft data. ECMWF has also begun to use varying uncertainty estimates for different types of radiosondes. All these changes improve the quality of ECMWF's forecasts. Further current developments include the use of solar radiation measurements from surface stations to verify predicted surface fluxes and the monitoring of radiosonde descent reports to see what use can be made of them.

Radiosondes

The change from alphanumeric to BUFR format requires significant software changes at the radiosonde stations and downstream. In return it makes it possible to report at much higher vertical resolution, providing the position at each level plus extra precision and metadata (*Ingleby et al.*, 2016). Figures 1 and 2 show how the provision of high-resolution reports has progressed, but there is still much to do. High-resolution reports were initially mainly available from Europe. In late 2015, Australian stations were added, and in the second half of 2017 most stations in the USA started sending high-resolution data. With contributions from other countries there are now some high-resolution reports from each continent. However, there are still large areas with no acceptable BUFR data. ECMWF thins the levels in the vertical (from often between 3,000 and 6,000 to about 350) before assimilation. ECMWF's use of 'significant levels' (turning points) in alphanumeric reports is not optimal (*Ingleby et al.*, 2016), so this provides an additional reason to move to high-resolution reports.

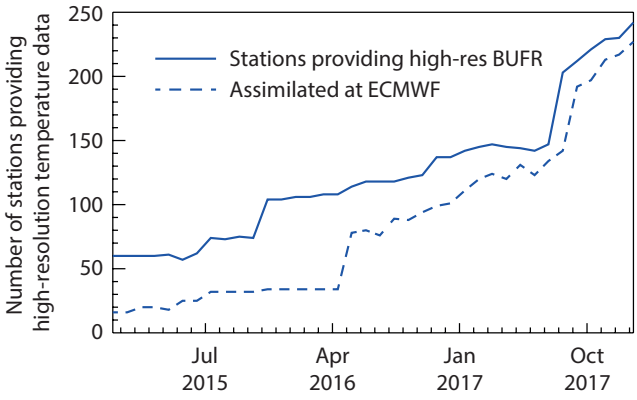

Figure 1 The number of land stations providing at least five high-resolution temperature profiles per month and the number of such stations assimilated at ECMWF. About 800 stations in total provide five or more temperature profiles per month in TEMP and/or BUFR format.

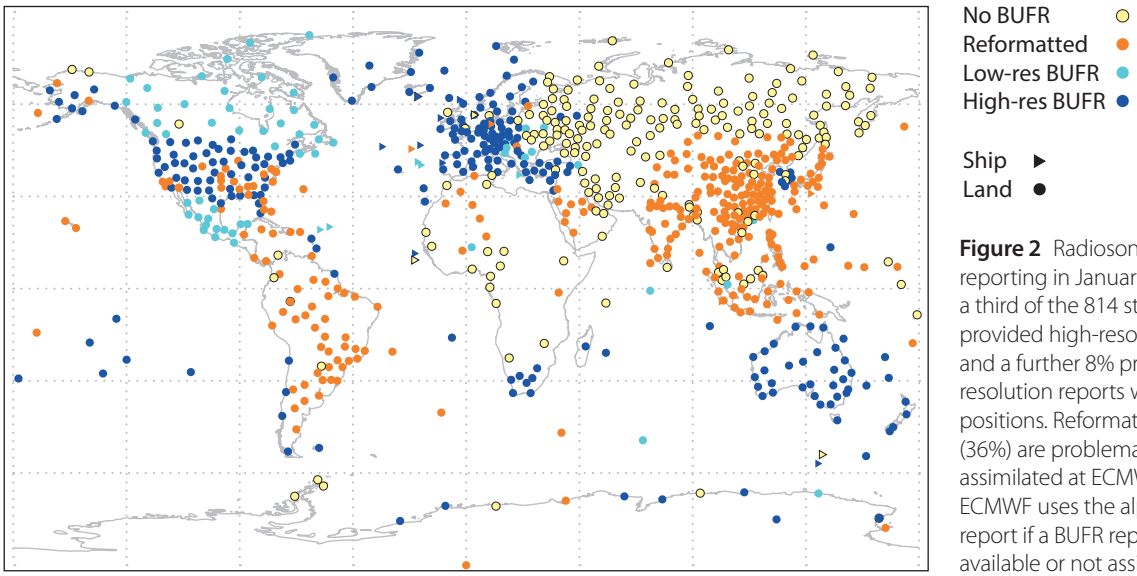

Figure 2 Radiosonde stations reporting in January 2018. Nearly a third of the 814 stations (31%) provided high-resolution reports and a further 8% provided low-resolution reports with drift positions. Reformatted TEMP reports (36%) are problematic and are not assimilated at ECMWF. In general, ECMWF uses the alphanumeric report if a BUFR report is not available or not assimilated.

When new BUFR bulletins are received at ECMWF, the data are monitored for a while before being assimilated. Occasionally changes to the decoding software are needed to cope with new features in the messages. Sometimes data producers are notified of problems in the messages. The rolling implementation in the assimilation is needed to ensure that ECMWF is using the BUFR reports before the alphanumeric reports cease to be distributed.

A detailed report (*Ingleby*, 2017; part of a contract for Vaisala Oyj) has been produced looking at the quality of different radiosonde types, mainly by investigating how the observations compare to a 12-hour forecast known as the background within the data assimilation system. Such observation-minus-background ('O–B') statistics can be used to compare the quality of different subsets of observations. The statistics vary with latitude and height and also, particularly for temperature and upper tropospheric humidity, by radiosonde type. Until recently the ECMWF assimilation system used the same observation uncertainty estimates for all radiosonde types, but in July 2017 a change was made to vary the uncertainty estimates and also reduce the default humidity uncertainties. As shown in Figure 3, this change has had a generally positive impact on forecast scores. Unfortunately there was an error in the scaling of the temperature uncertainties, which will be corrected in the next IFS upgrade planned for later this year (IFS Cycle 45r1).

One advantage of BUFR radiosonde reports is that the position at each level can be reported. A radiosonde ascent takes about two hours and, as shown in Figure 4, during that time the radiosonde can move horizontally by 200 km or more. Only launch location is available for old-style TEMP data, so in data assimilation systems the profile has generally been treated as vertical and instantaneous. As the resolution and accuracy of data assimilation systems improve, this approximation becomes less appropriate and better treatment of the drift can improve analysis and forecast performance (*Laroche & Sarrazin*, 2013). Analogous improvements have been made to account for the slant path of satellite soundings (*Bormann*, 2017).

Processing of radiosonde drift (for stations where ECMWF is assimilating BUFR data) will become operational in IFS Cycle 45r1. For technical reasons the processing splits each profile into 15-minute intervals, and observations from each interval are treated as vertical and instantaneous. The intervals may be shortened in the future. As shown in Figure 5, the change improves stratospheric wind and temperature O–B standard deviation values by between 5 and 10% for stations reporting drift positions. In the upper troposphere, wind O–B standard deviation values are improved by several per cent. Biases are also improved, especially for wind. In the extratropics there are improvements of about 1% in 50 hPa wind root-mean-square verification against analyses for two-day forecasts. At longer range there are smaller improvements in the troposphere, which are more apparent in the southern hemisphere than in the northern hemisphere. These modest forecast improvements (not shown) were

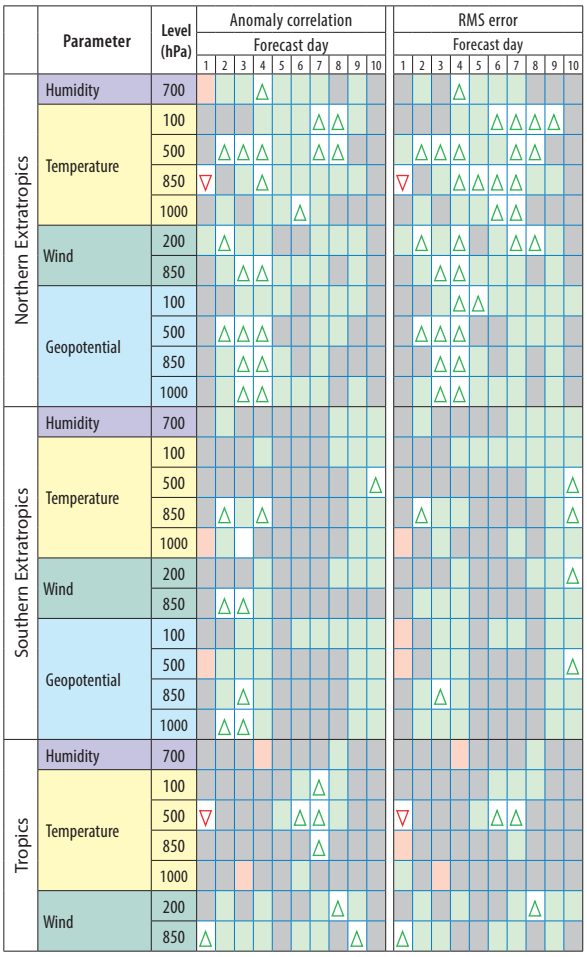

Figure 3 Scorecard comparing forecasts with varying observation uncertainty by radiosonde type (experiment A) with forecasts without varying observation uncertainty (experiment B) over the period July to September 2015.

obtained when about 15% of radiosonde stations were reporting drift positions – the benefits should be greater when more stations take full advantage of the new features in BUFR (in the year since then the proportion has increased to 31%).

Over the last two years there have also been changes to radiosonde humidity conversions to improve consistency between assimilated radiosonde data and model fields in the upper troposphere (*Ingleby*, 2017). In addition, a relaxation of the quality control has been introduced to reduce rejections of radiosonde temperature and wind data in the stratosphere.

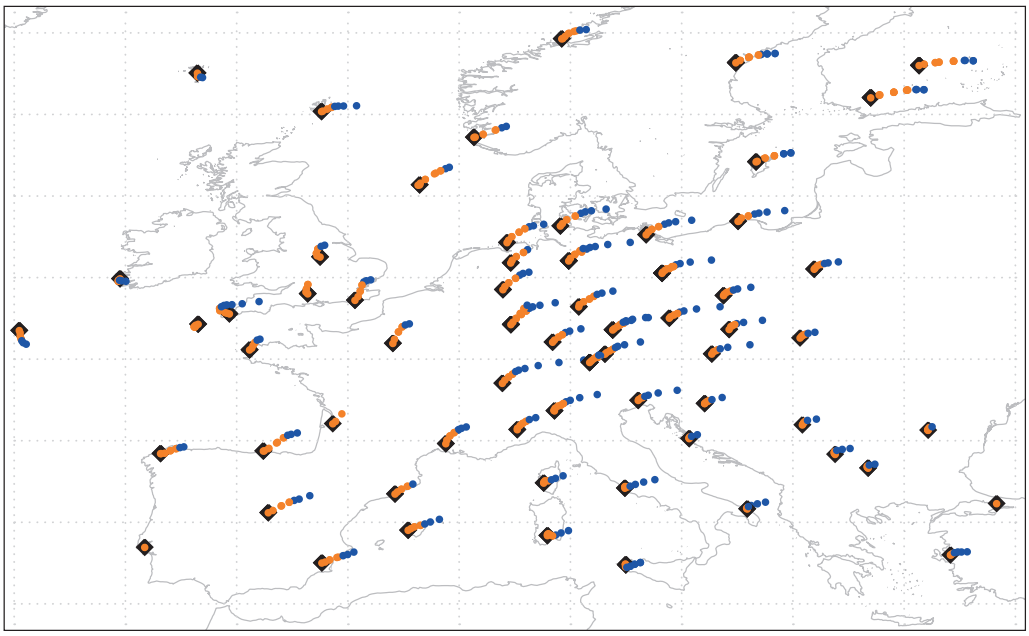

Figure 4 Radiosonde drift over Europe in the 12 UTC analysis on 21 November 2016. Only BUFR reports are shown. A few of these were reformatted and do not include drift positions. Positions are shown every 15 minutes.

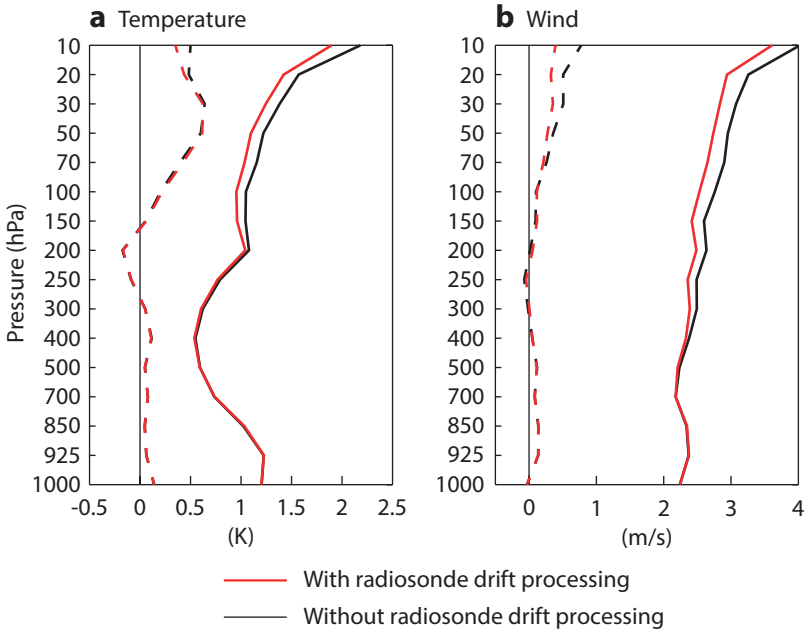

Figure 5 Standard deviation (solid lines) and mean (dashed lines) radiosonde observation-minus-background (O–B) statistics for European stations with and without drift processing for (a) temperature and (b) zonal (east–west) wind, for November 2016 to February 2017. Meridional (north–south) wind has similar statistics to zonal wind, and results for Australia plus New Zealand are broadly similar but with slightly less improvement in the standard deviation.

Dropsondes (dropped from aircraft) are available intermittently, often in the vicinity of tropical cyclones (TCs). Typically they improve TC analyses and forecasts, but there are cases where they are badly handled and degrade the TC analysis. The quality control and weighting of dropsonde data was recently made more robust (*Bonavita et al.*, 2017). Particularly for profiles near the eye-wall of a storm, taking into account the location of the dropsonde at each level may be very important. Test high-resolution BUFR files from US dropsondes with position information at each level have been obtained and impact experiments will be run in the coming months.

Aircraft

Aircraft observations are very valuable for global NWP. However, the temperature values are typically biased by between 0.2 and 0.5˚C, depending on the aircraft. In November 2011, ECMWF implemented a variational bias correction scheme similar to the one applied to satellite soundings. It uses the aircraft tail identifier as a predictor for bias for all observations from each modern-style AMDAR (Aircraft Meteorological Data Relay) report. But it is not applied to the smaller number (5 to 10% of the total) of old-style voice reports (AIREPs), where it is not possible to identify the aircraft.

A new version of the bias correction scheme has been developed for all aircraft data types and will become operational in IFS Cycle 45r1. The new version takes account of the fact that ascent, descent and cruise aircraft temperature biases vary slightly. It does this by including

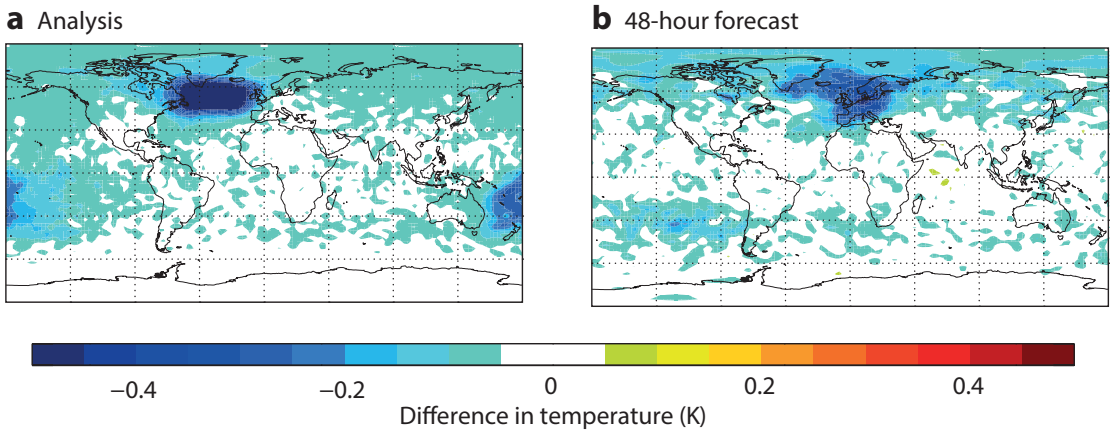

Figure 6 Mean differences in temperature at 200 hPa averaged over 50 days in June–July–August 2016 using the new and the old bias correction scheme ('new' minus 'old') for (a) the temperature analysis at 200 hPa and (b) 48-hour forecasts at 200 hPa. Blue shading means the new bias correction cools the analysed/predicted atmosphere.

three aircraft-specific bias predictors (cruise, ascent and descent) rather than just one. Three methods to represent the flight phase in the variational bias correction scheme have been tested. The first uses *dp/dt* (pressure change) computed from successive aircraft measurements, the second uses *dz/dt* (height change) computed from successive aircraft measurements, and the third method uses the cruise/ascent/descent status provided with the AMDAR aircraft measurement to set a fixed ascent/descent rate. The best results are obtained when *dz/dt* is used, which is as one would expect, so this method was selected.

The new version of the scheme has also been used to show that it is beneficial to perform a bulk bias correction of the old-style AIREP temperature observations, because the biases are fairly uniform. The old-style AIREP observations are concentrated in the North Atlantic flight routes between Europe and the USA, where they account for up to 50% of cruise level aircraft reports. Figure 6 shows how the bulk bias correction of old-style AIREP results in up to 0.5˚C mean cooling of the analysis and forecasts at 200 hPa, near cruise level. The bias correction of old-style AIREP temperature observations has been applied to the new ERA5 reanalysis, leading to improvements compared to ERA-Interim in the North Atlantic region.

Since November 2017, almost all the aircraft that provide old-style AIREPs have provided AMDARs as well (but not exactly at the same positions or using the same identifier, making thinning difficult to handle). With the tail identifier available, we can now bias-correct these aircraft data like other AMDARs. This has had a similar effect on 200 hPa temperatures to that shown in Figure 6. With the availability of the data in AMDAR format and because the operational analysis is not yet able to bias-correct the old-style AIREP temperature data, it was decided to stop assimilating the uncorrected AIREP temperatures from 10 January 2018.

As part of the IFS Cycle 45r1 upgrade of aircraft data assimilation, aircraft observations will be rejected very close to airports (lowest 30 hPa) due to large biases in such locations, which are particularly big for temperatures over runway tarmac. Data thinning will also be reduced by a factor of two to 35 km horizontally and 7.5 hPa vertically, to be more in line with the forecast and analysis resolution upgrade introduced in March 2016. Figure 7 shows that the reduced thinning results in 10 to 20% more aircraft data being used at around 850 hPa and at or near cruise level.

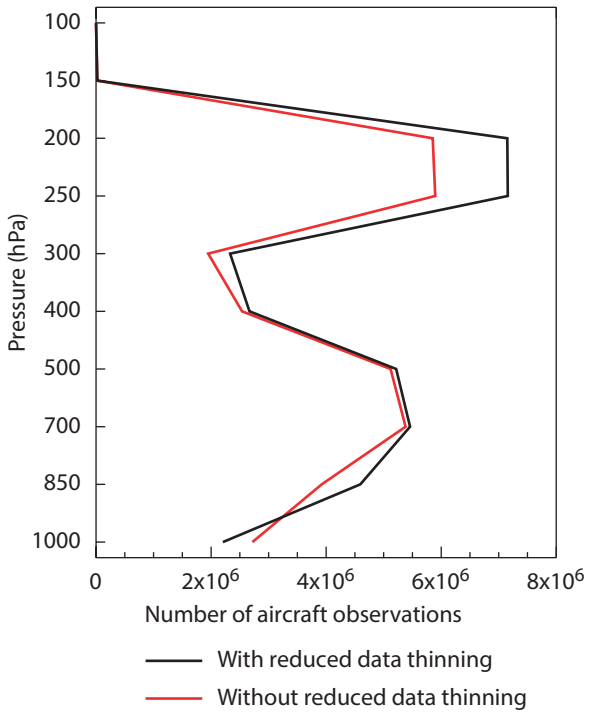

Figure 7 Comparison of the number of aircraft observations as a function of altitude (expressed in terms of pressure) with and without reduced observation thinning, based on data for June to August 2016. Less data is used with reduced thinning near the surface due to the rejection of data in the lowest 30 hPa.

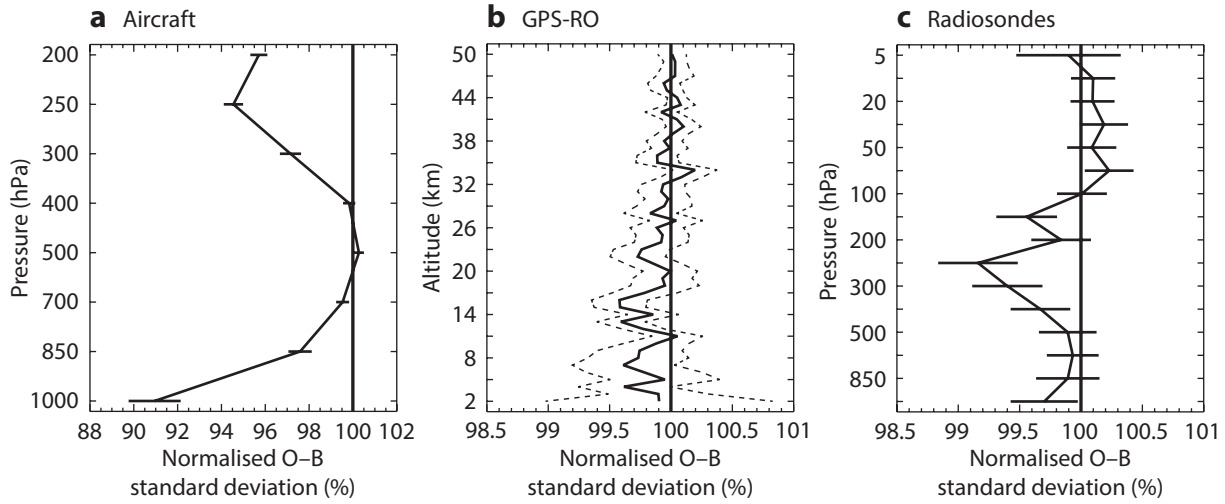

Figure 8 Normalised observation-minus-background (O–B) standard deviation for (a) temperature data from aircraft, (b) normalised bending angle for GPS-RO and (c) temperature data from radiosondes when improved bias correction and thinning of aircraft data is applied. Sections of the lines that lie to the left of the 100% mark denote improved O–B statistics. Horizontal bars and dotted lines represent 95% confidence intervals.

The total effect of the improved bias correction and thinning of the aircraft data improves the analysis and forecasts. As shown in Figure 8, the changes reduce the standard deviation O–B values for not just aircraft and radiosonde temperature observations, but also GPS-RO bending angle data. The bending angle is related to temperature, and also to humidity at lower levels. There is also a reduction of about 0.1 K in radiosonde temperature O–B biases at 100–300 hPa (not shown).

In recent months wind errors for certain aircraft have been noted over the North Atlantic and some of these have been placed on a reject list. We understand that these are B787 aircraft and have contacted the data providers (in the USA) to try to resolve the problem in the longer term.

Surface

Interest in solar radiation measurements is increasing, partly because of the growth in photovoltaic electricity generation. Radiation measurements are also useful for validating predicted surface radiation fluxes, which are strongly affected by cloud forecasts. For many years NWP centres have performed verification of cloud forecast skill against surface station data based on SYNOP observations of total cloud cover and, where available, low, medium, and high cloud cover. However, cloud cover is not a particularly well-defined quantity, especially for cirrus clouds. More recently ECMWF has verified predicted surface radiation fluxes using data from Baseline Surface Radiation Network (BSRN) stations. These are comprehensively equipped but much less numerous than SYNOP stations, and they can take months to provide data. Over 600 SYNOP stations, mainly from Europe, now report hourly solar radiation measurements in real time (Figure 9). Smaller numbers report diffuse solar and longwave measurements. Work is under way to add these to the verification of predicted solar radiation. As can be seen in Figure 9, the network of SYNOP stations reporting radiation measurements is much denser in some parts of Europe than in others, and there are no reports at all from a number of areas. Where countries are making radiation measurements at SYNOP stations, we would urge them to add them to the real-time reports.

ECMWF applies surface pressure bias correction to a small proportion of stations (about 6%). The corrections are updated every 12 hours and sometimes they change too rapidly, usually during the passage of a storm. Work is under way to avoid rapidly changing corrections that do not represent observation biases.

In July 2016, ECMWF started assimilating surface pressure and some wind data from BUFR buoy reports before most alphanumeric reports ceased in November 2016.

Ongoing work

The WMO has announced the replacement of five-digit station identifiers with more complex WMO Integrated Global Observing System (WIGOS) station identifiers. In the short term this means that many software systems will need to change. In the longer term it should enable ECMWF to use reports from many more surface stations – some run by weather services, some run by other agencies. In addition, work is still under way to process new BUFR templates (such as that for dropsonde data). As previously reported in this Newsletter (*Prates & Richardson*, 2016), ECMWF is taking part in a WMO data quality monitoring pilot project concentrating on surface and radiosonde data to support the future implementation of a WIGOS Data Quality Monitoring System (WDQMS).

Vaisala RS92 is still the most used type of radiosonde worldwide, but that is changing rapidly as Vaisala withdraws the RS92 in favour of the newer RS41. The ECMWF radiosonde temperature/humidity bias correction currently uses RS92 as a reference. It will soon start to use an average

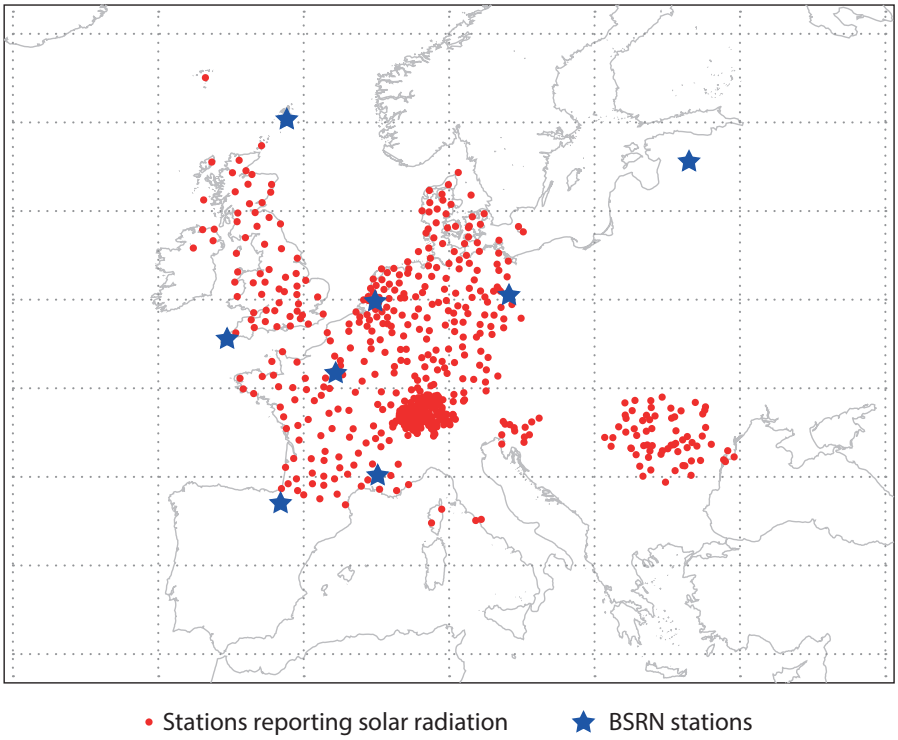

Figure 9 Map of SYNOP stations reporting solar radiation in November 2017, showing the 556 stations located in Europe. There are another 53 stations elsewhere. Also shown are the eight European Baseline Surface Radiation Network (BSRN) stations used in the verification of predicted surface radiation fluxes.

of RS92 and RS41 data and will switch off the humidity bias correction for RS41 radiosondes. In a separate development, test 'radiosonde descent' reports are being received from several stations. These contain data after balloon burst and are more variable in quality than ascent profiles. However, since there is very little additional cost, they are of interest. ECMWF will start to monitor these reports before deciding whether or not to use the data, and whether any extra processing or checks are needed.

For EUMETNET we performed a study of the impact of pressure data from drifting buoy reports on NWP and also the effect of the report density. A paper on this has been accepted by the journal *Atmospheric Science Letters*. ECMWF is also providing input to an international team considering radiosonde reporting including a) recommendations for target height and b) whether to allow more flexibility in reporting times (traditionally 00 and 12 UTC).

In situ reports are varied and valuable. To make the best use of them, work to introduce new reports and variables is needed, as is ongoing monitoring of operational data. As this article illustrates, progress is being made on many fronts. Among recent advances, the ability to account for radiosonde drift stands out as a particularly significant development since it addresses a long-standing approximation in the processing of atmospheric in situ observations.

FURTHER READING

Bonavita, **M.**, **M. Dahoui**, **P. Lopez**, **F. Prates**, **E. Holm**, **G. De Chiara**, **A. Geer**, **L. Isaksen** & **B. Ingleby**, 2017: On the initialization of Tropical Cyclones. *ECMWF Technical Memorandum* **No. 810**.

Bormann, **N.**, 2017: Assimilating satellite data along a slanted path. *ECMWF Newsletter* **No. 153**, 32–36.

Ingleby, **B.**, 2017: An assessment of different radiosonde types 2015/2016. *ECMWF Technical Memorandum* **No. 807**.

Ingleby, **B.**, **E. Fucile**, **T. Kral**, **D. Vasijevic** & **L. Isaksen**, 2014: Use of radiosonde and surface observations provided in BUFR format. *ECMWF Newsletter* **No. 140**, 10–11.

Ingleby, **B.**, **P. Pauley**, **A. Kats**, **J. Ator**, **D. Keyser**, **A. Doerenbecher**, **E. Fucile**, **J. Hasegawa**, **E. Toyoda**, **T. Kleinert**, **W. Qu**, **J. St James**, **W. Tennant** & **R. Weedon**, 2016: Progress towards high-resolution, real-time radiosonde reports. *Bull. Amer. Meteor. Soc.*, **97**, 2149–2161.

Laroche, **S.** & **R. Sarrazin**, 2013: Impact of Radiosonde Balloon Drift on Numerical Weather Prediction and Verification. *Weather and Forecasting*, **28**, 772–782.

Prates, **C.** & **D. Richardson**, 2016: ECMWF takes part in WMO data monitoring project. *ECMWF Newsletter* **No. 148**, 19.

doi:10.21957/ab84rhs9t5

A new radiation scheme for the IFS

ROBIN J. HOGAN, ALESSIO BOZZO

Radiation is a fundamental process that drives atmospheric flows at all scales. It is key to both improving short-range surface temperature forecasts and meeting ECMWF's strategic aim of pushing the boundaries of predictability at medium-range and longer timescales. In 2007, the 'McRad' radiation scheme became operational in ECMWF's Integrated Forecasting System (IFS). It incorporated two major advances: very accurate gas optical properties in both the shortwave and longwave from the Rapid Radiative Transfer Model for general circulation models (RRTM-G), and the Monte Carlo Independent Column Approximation (McICA) for efficient treatment of cloud sub-grid heterogeneity. Many weather and climate models have since incorporated one or both of these advances.

Two shortcomings of McRad have motivated the recent development of a new ECMWF radiation scheme, 'ecRad'. Firstly, *flexibility*: to facilitate ongoing scientific development, we need the ability to swap individual components of the radiation scheme for faster and more accurate ones, but the non-modular design of McRad makes this very difficult.

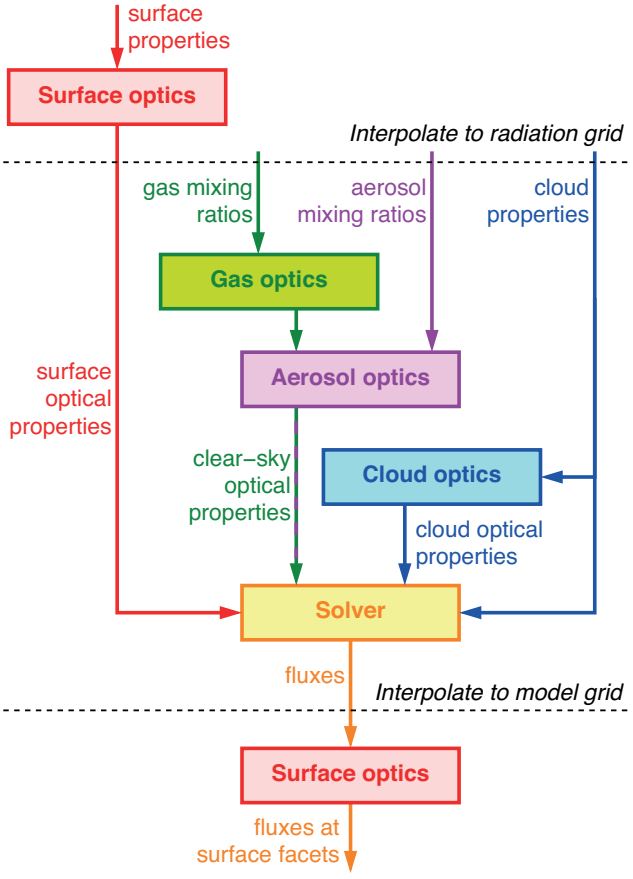

Figure 1 Schematic illustrating the five main components of ecRad (differently coloured boxes) and the flow of data between them (arrows).

Secondly, *efficiency*: the large number of spectral intervals (252) required by RRTM-G made McRad 3.5 times slower than its predecessor. The result is that the radiation scheme has to be run on a much coarser grid than the rest of the model, and in all operational model configurations except high-resolution forecasts (HRES) we only call the radiation scheme every 3 hours. In HRES the scheme is called every hour.

The new radiation scheme ecRad, which became operational in July 2017 (IFS Cycle 43r3), is faster and more flexible. It uses a new implementation of McICA that is less noisy in partially cloudy conditions. Improvements in longwave radiative transfer reduce biases in temperature profiles. As implemented in IFS Cycle 43r3, ecRad brings slight improvements in forecast skill. Its modular structure facilitates radiative transfer research and opens the door to more substantial improvements in forecast skill in the future.

Modular structure

The new scheme is made up of five largely independent components. The first is taken from McRad while the others (amounting to 16,000 lines of code) are new. The components are shown in Figure 1 along with the flow of data between them. They are:

1. **Gas optics**: this component computes gas absorption and scattering in each spectral interval and dictates the spectral resolution, which is one of the main factors determining the computational cost of the entire scheme. Currently only RRTM-G is available, but we plan to add alternatives in future in order to give the user the option of choosing a different trade-off between accuracy and cost.
2. **Aerosol optics**: this component adds the aerosol contribution to the clear-sky optical properties. The number of aerosol species is run-time configurable with optical properties provided by a NetCDF configuration file. In this framework we are able to support various types of climatological aerosol distribution as well as prognostic aerosol schemes including the latest 15-species version of the IFS bulk aerosol scheme.
3. **Cloud optics**: new parametrizations are available in addition to those operational in McRad. For liquid clouds, the older Slingo scheme had been found to overpredict optical depth, so the ecRad default is a parametrization adapted from that used in the UK Met Office radiation scheme. For ice clouds, the Fu scheme is still used, but alternative schemes based on more recent measurements of ice size distributions and scattering patterns are undergoing testing.
4. **Solver**: this component merges clear-sky and cloudy optical properties, accounting for cloud fraction, heterogeneity and overlap, and solves for the profile of fluxes in each spectral interval. McRad had only one solver: McICA without longwave scattering. Three solvers are available in ecRad. Operationally we use a new implementation of McICA that is more efficient,

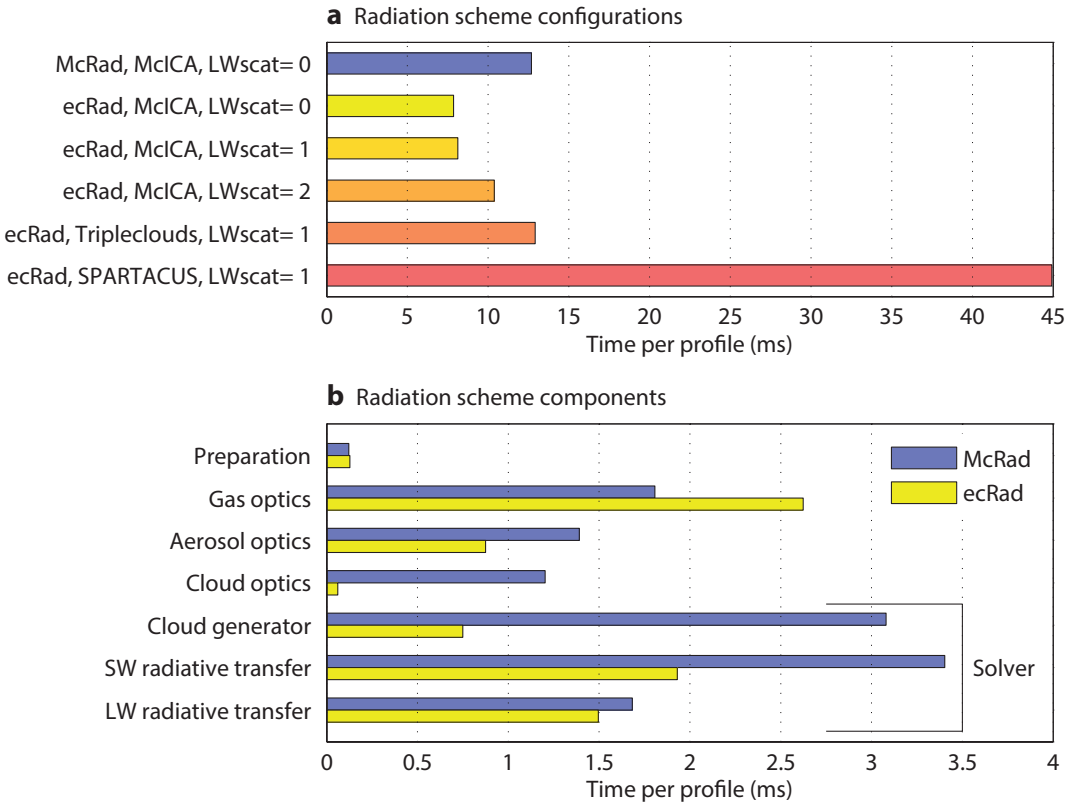

Figure 2 Computational cost of (a) various configurations of the radiation scheme, expressed in terms of the time needed to run it per atmospheric profile, where the labels on the left indicate the scheme name, solver name and longwave scattering configuration (0 = no longwave scattering, 1 = scattering by clouds only, 2 = scattering by clouds and aerosols), and (b) the first two configurations broken down by different radiation scheme components.

generates less stochastic noise and includes the option to turn on longwave scattering. Also available are the Tripleclouds and SPARTACUS solvers, discussed below. In addition, we have added the ability to choose between three cloud overlap schemes, and to change both the width and the shape of the sub-grid probability density function of cloud water content.

5. **Surface optics**: development of this component is in progress. It is intended to represent the radiative interaction with complex surfaces, such as urban areas and forests; the theoretical basis for the latter was described by *Hogan et al.* (2018). It will run on the full model grid rather than the lower-resolution radiation grid, and compute radiative fluxes at each facet of the surface. This will enable the energy budget to be treated separately for the streets, walls and roofs of the planned 'urban tile', and likewise for the vegetation and ground of forest tiles.

Greater efficiency

Figure 2 shows the computational cost of various versions of the radiation scheme when run in the coupled IFS at TCo1279 resolution (corresponding to a grid spacing of 9 km). The top two bars of the top panel show that ecRad is around 35% faster than McRad when in a similar configuration (McICA solver with no longwave scattering); this is the configuration used operationally in IFS Cycle 43r3. The lower panel shows a breakdown of the computational cost by component, highlighting the impact of individual optimisations. An overarching change is to make spectral interval rather than atmospheric column the fastest varying dimension in optical-property arrays. This improves performance overall since conditional operations (which inhibit vectorisation) depend on the presence of cloud or whether the sun is above the horizon, factors that are functions of atmospheric column but not spectral interval. For the moment this makes gas optics slower because this component has not yet been recoded, so the output arrays have to be permuted, but this is more than compensated for by a speed-up in other components.

The job of the cloud generator in a McICA solver is to stochastically produce a different cloud-profile realisation for each spectral interval, consistent with the specified cloud overlap and horizontal heterogeneity. The ecRad cloud generator is much faster because it has been devised to use far fewer random numbers. An even greater speed-up has been achieved in computing cloud optical properties: McRad recomputed them in each of the 252 spectral intervals, when in fact it is only necessary to compute them in the 30 broader spectral bands in which the coefficients of the cloud optics parametrizations are defined.

Radiation now occupies a very small fraction of model time: with ecRad it is only 3.5% in coupled simulations at a resolution of TCo1279 with the radiation scheme called every hour. This figure includes the cost of interpolating back and forth between the model grid and the radiation grid. This is a large improvement on the 19% reported when McRad was implemented in the uncoupled HRES in 2007. The efficiency gain is a consequence of several factors in addition to ecRad optimisations: (1) the longer model time step in 2007, while radiation was still called every hour, (2) the additional cost of the ocean model (9% of wall-clock time in HRES), and (3) in 2007 radiation was run on a grid with six times fewer grid points than the rest of the model, compared to ten times fewer now. *Hogan et al.* (2017) have demonstrated that the forecast degradation due to the coarser grid is very small, partly thanks to the use of approximate radiation updates on the finer model grid that mitigate problems at coastlines.

Better McICA solver

A downside to the McICA approach is that it can produce significant stochastic noise in atmospheric heating rates. Even though 252 realisations of the cloud profile are generated, many are in absorbing parts of the spectrum where the cloud radiative effect is not significant; indeed, only around 40% of the spectral intervals have a clear-sky optical depth less than 3. Moreover, the McRad implementation of McICA exacerbates the noise in partially cloudy situations, since many of the stochastic profiles generated are then cloud-free.

The problem is illustrated in Figure 3: a real profile of shortwave and longwave heating rates in a partially cloudy column extracted from the 137-level IFS. We compare the McRad and ecRad implementations of McICA to the alternative 'Tripleclouds' solver available in ecRad, which is considerably more expensive than McICA (see Figure 2) but generates no stochastic noise. The noise in the McRad implementation is large, with up to 5 K/day errors in the longwave heating rate compared to 'Tripleclouds', which is used as a proxy for the truth. In all model configurations except HRES, the radiation time step is 3 hours, so these erroneous temperature tendencies accumulate over a number of model time steps.

The ecRad implementation of McICA does exhibit noise, but the amplitude of errors in Figure 3 is significantly lower than for McRad. This has been achieved thanks to two improvements. Firstly, total cloud cover is now computed deterministically from the cloud fraction profile and the overlap rules, so removing stochastic noise in cloud cover (even though the cloud profiles within the cloudy part of the gridbox are still stochastically generated). Secondly, we make use of the fact that clear-sky radiation calculations (i.e. fed by the same atmospheric profiles except with the clouds removed) are already performed for diagnostic purposes, so we can use the cloud generator to produce only cloudy profiles, and then compute the total-sky flux profile as a weighted average of the clear and cloudy profiles. This leads to much better sampling of the cloudy part of the column in partially cloudy conditions. Details were given by *Hogan & Bozzo* (2016).

Improvements in longwave radiative transfer

The longwave part of ecRad has been improved: the two-stream radiative transfer equations are now solved exactly under the assumption that the Planck function varies linearly within each model level, while the treatment in McRad is more approximate. As shown in *Buizza et al.* (2017), this tends to reduce extrema in the temperature profile, warming the tropopause by around 0.5 K and cooling the stratopause by around 1 K. Both of these changes reduce existing biases.

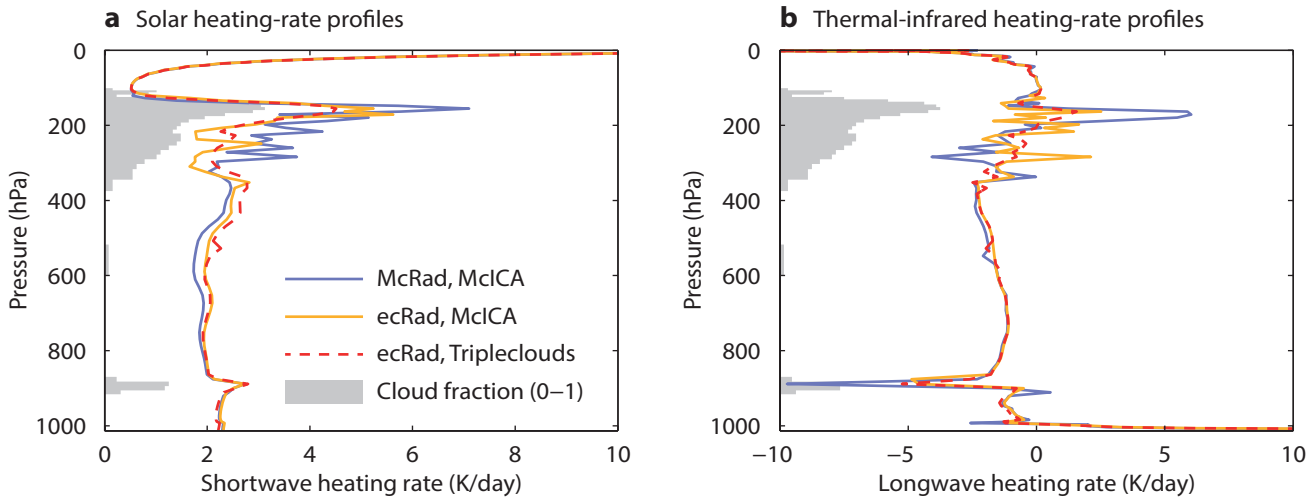

Figure 3 Profiles of (a) instantaneous solar heating-rates and (b) instantaneous thermal-infrared heating-rates for a single column of the atmosphere, comparing the previous McRad scheme (with noise of up to 5 K per day), the ecRad scheme with the reduced-noise McICA solver, and ecRad with the computationally more expensive but noise-free Tripleclouds solver. The grey shading indicates the location of clouds.

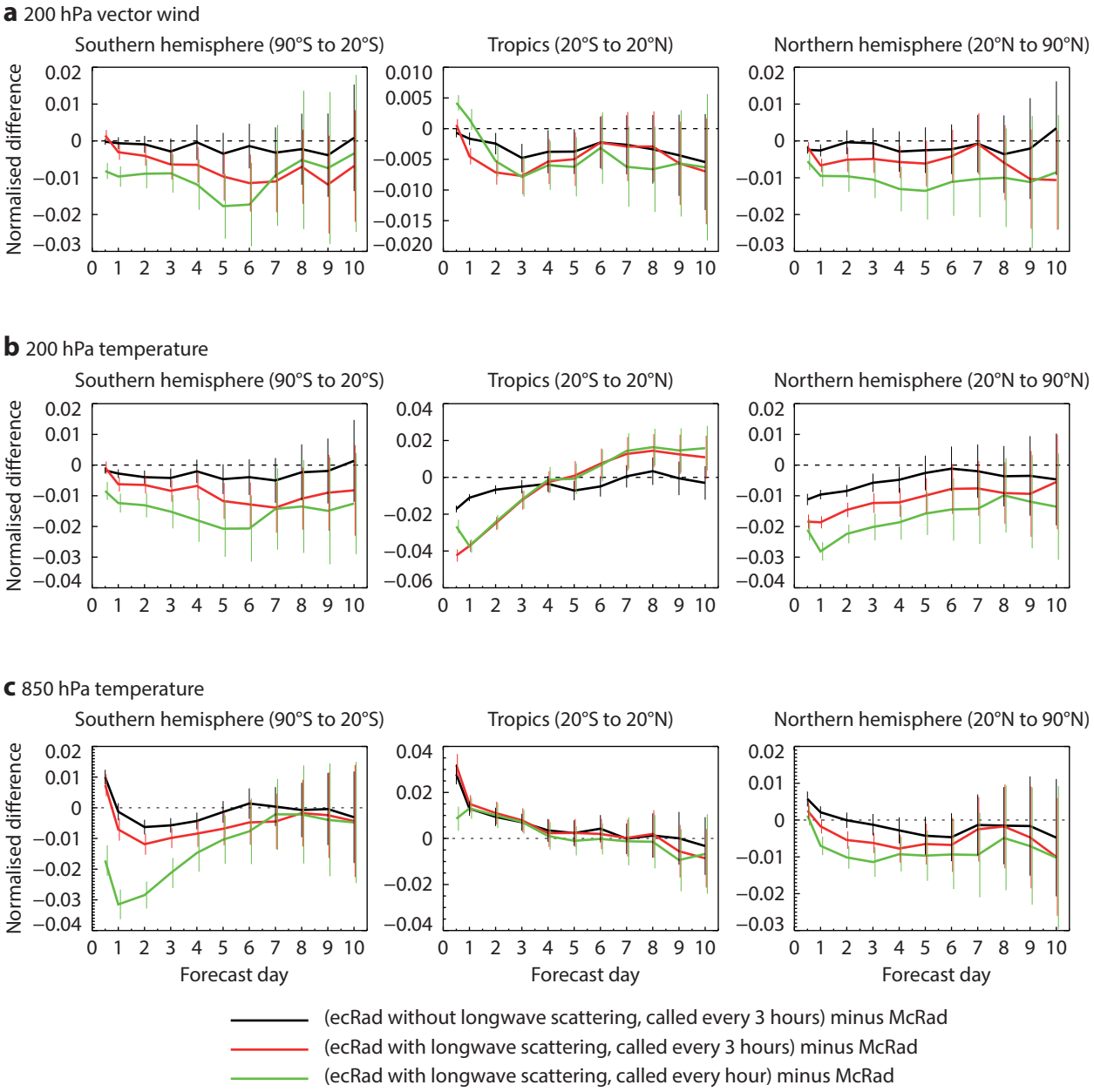

Figure 4 Normalised change to root-mean-square error in (a) 200 hPa vector wind, (b) 200 hPa temperature and (c) 850 hPa temperature when switching from the McRad radiation scheme to three configurations of the ecRad scheme. A value of –0.01 indicates a reduction in error of 1%. The uncoupled forecasts were performed at TCo399 resolution from June to September 2016 and evaluated against the then operational forecasts (IFS Cycle 41r2).

Turning on longwave scattering in ecRad is under testing for one of the next operational IFS cycles. Physically, the introduction of scattering results in optically thick clouds no longer behaving as a black body (with an emissivity of one) but rather reflecting a certain fraction of incident radiation. This change in turn reduces top-of-atmosphere outgoing longwave radiation and increases surface downwelling longwave radiation. Unfortunately, inclusion of scattering doubles the cost of the longwave solver and increases the total cost of ecRad by 32% (the difference between the second and fourth bars in the top panel of Figure 2). But in practice only longwave scattering by clouds is important, while for aerosols it can be neglected. This enables not only the clear-sky part of the calculation to use the no-scattering assumption, but also the layers above the highest cloudy layer in the all-sky part of the calculation. Thus longwave scattering by clouds may be included with only a 3% increase in the total cost of the scheme (the difference between the second and third bars in the top panel of Figure 2).

Impact on forecasts

The impact of various configurations of ecRad on medium-range forecasts skill is summarised in Figures 4 and 5 for

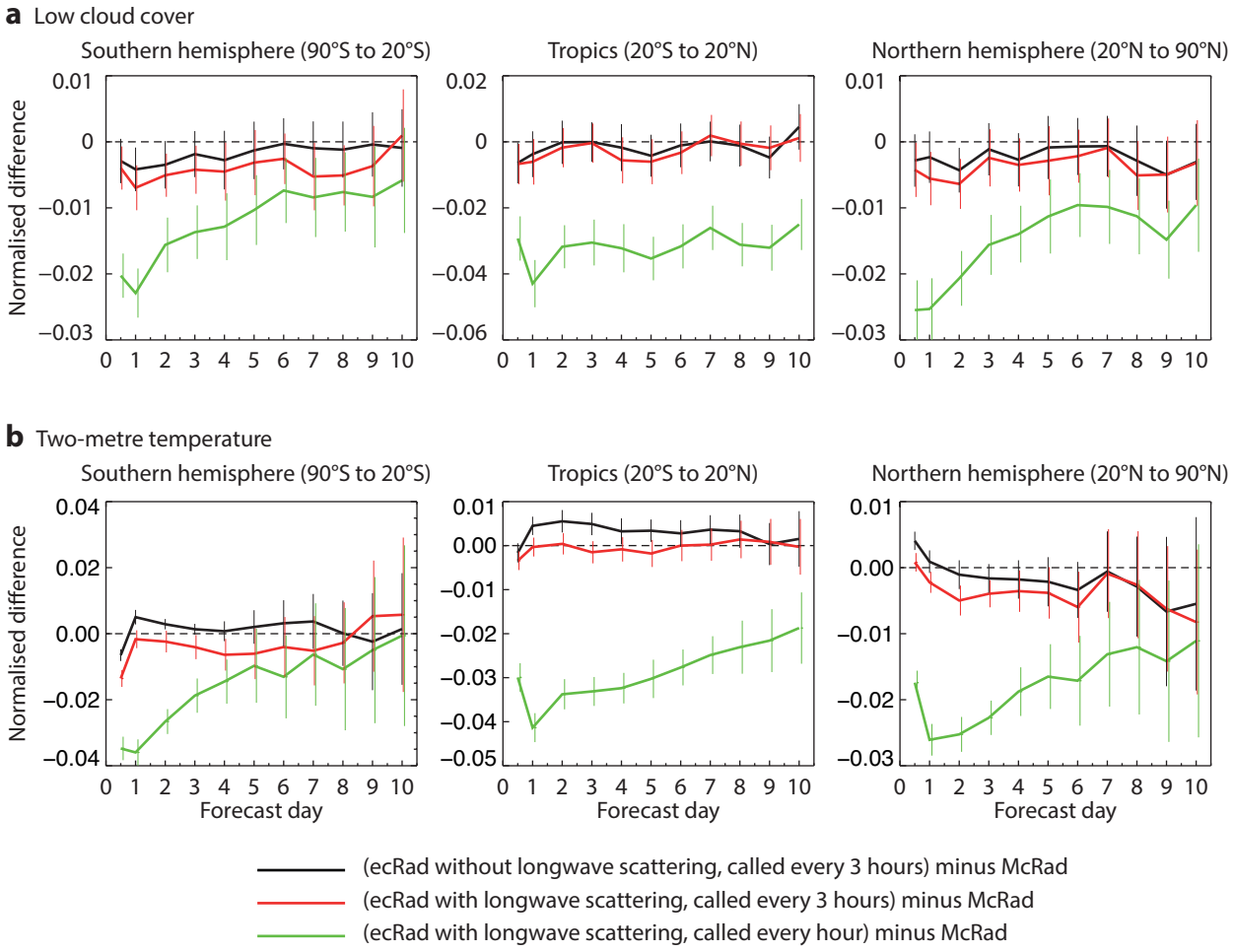

Figure 5 As Figure 4 but showing the change to root-mean-square forecast error for (a) low cloud cover and (b) 2-metre temperature.

a 3-hour radiation time step, which is used in ensemble forecasts (ENS). The ecRad configuration operational in IFS Cycle 43r3 includes the reduced-noise McICA solver and a better solution to the longwave equations, but does not include longwave scattering. Its impact on temperature and wind compared to McRad is overall slightly positive. The introduction of longwave scattering yields a further extratropical improvement of around 1% at all forecast lead times. Note that McRad included an approximate treatment of longwave scattering, but it was only implemented for ice clouds and only affected clouds of low to moderate optical depth.

Larger improvements in skill are potentially available indirectly from the greater efficiency of ecRad, by reinvesting the time saved into calling the radiation scheme more frequently than every 3 hours. A reduction in the ENS radiation time step to 1 hour to align it with HRES is under consideration for one of the next operational IFS cycles. Figure 5 shows that in deterministic forecasts this significantly improves 2-metre temperatures at all lead times, especially in the tropics, and appears to be associated with an improvement in the prediction of low cloud cover. As shown by *Hogan et al.* (2017), the same improvement is obtained in ENS skill scores, and more than half of the improvement could be obtained by reducing the radiation time step to 2 hours rather than 1 hour.

Facilitating radiation research

The flexibility and capabilities of ecRad make it an excellent tool for radiative transfer research. For example, the availability of the SPARTACUS solver (*Hogan et al.*, 2016) makes the IFS the only global model capable of representing 3D radiative effects at a reasonable computational cost. This makes it possible to estimate the global impact of 3D radiative transfer. Our current best estimate is that 3D radiative transfer increases longwave and shortwave downwelling fluxes at the surface each by around 1 W/m^2, which in turn warms the land surface by on average 0.5 K in 1-year free-running coupled IFS simulations. This is of a similar order to the impact of changing the specification of cloud overlap and horizontal heterogeneity within observational uncertainty.

The introduction of ecRad has also made it easier to test alternative aerosol formulations in the radiation scheme. This has facilitated the introduction of a new aerosol climatology, based on data provided by the

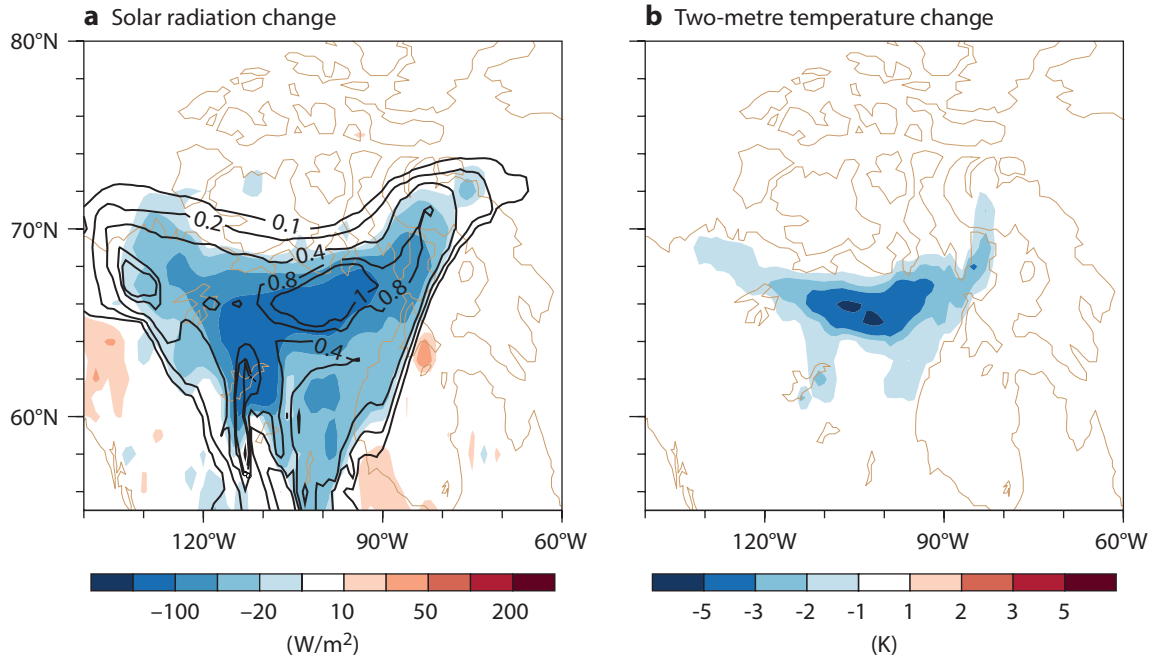

Figure 6 Impact of prognostic aerosols from the IFS bulk aerosol scheme on forecasts initialised at 00 UTC of (a) surface downwelling solar radiation averaged over the first full day of the forecast over Canada, and (b) 2-metre temperature averaged over 0600–1800 local time (forecast lead times of 12–24 hours), for 14 August 2017 when extensive forest fires occurred in Northern Canada. The contours in the left-hand panel show the 24-hour average optical depth of biomass burning aerosols.

Copernicus Atmosphere Monitoring Service (CAMS), in IFS Cycle 43r3 (*Buizza et al.*, 2017). It is also underpinning ongoing development of the prognostic aerosol scheme in the IFS, which is used for global CAMS forecasts. The interaction between prognostic aerosols and radiation will shortly be turned on for operational CAMS forecasts, and will be in the next CAMS reanalysis. Aerosol variability can influence surface temperature, particularly during intense events such as volcanic eruptions, dust storms and forest fires. For example, the wildfires that occurred in the North-West Territories of Canada during August 2017 were amongst the largest by both extent and total carbon emission in the region over the last decade. Figure 6 shows the difference between forecasts with prognostic and climatological aerosols being fed to the radiation scheme, revealing that the thick smoke plume on 14 August reduced surface solar radiation by 50–100 W/m^2, which in turn reduced mean daytime temperatures in the area by up to 5 K.

An offline version of ecRad has been available for non-commercial use under the terms of the OpenIFS licence since February 2017. It now has users in Algeria, China, France, Germany, the United Kingdom and the United States. It is being used at the University of Reading to generate greenhouse-gas and aerosol radiative forcing products from the CAMS interim Reanalysis (CAMSiRA), and at the University of Leipzig and Laboratoire de Météorologie Dynamique in Paris to improve our understanding of the radiative properties of clouds observed by aircraft and satellites. It has also been implemented in the limited-area Meso-NH model.

Outlook

A number of ecRad developments are planned for the coming years. A surface component will be added that can rigorously treat radiative interactions with complex surfaces, such as urban areas and forests. We plan to upgrade the treatment of cloud properties, aiming for consistency with the assumptions made in the cloud, convection and assimilation schemes, and to introduce the radiative effects of rain and convective cloud. We also plan to develop and test an alternative, faster gas optics scheme with fewer spectral intervals.

FURTHER READING

Buizza, **R.**, **P. Bechtold**, **M. Bonavita**, **N. Bormann**, **A. Bozzo**, **T. Haiden**, **R. Hogan**, **E. Holm**, **G. Radnoti**, **D. Richardson** & **M. Sleigh**, 2017: IFS Cycle 43r3 brings model and assimilation updates. *ECMWF Newsletter* **No. 152**, 18–22.

Hogan, **R.J.** & **A. Bozzo**, 2016: ECRAD: a new radiation scheme for the IFS. *ECMWF Technical Memorandum* **No. 787**.

Hogan, **R.J.**, **S. A. K. Schäfer**, **C. Klinger**, **J.-C. Chiu** & **B. Mayer**, 2016: Representing 3D cloud-radiation effects in two-stream schemes: 2. Matrix formulation and broadband evaluation. *J. Geophys. Res.*, **121**, 8583–8599.

Hogan, **R.J.**, **M. Ahlgrimm**, **G. Balsamo**, **A. Beljaars**, **P. Berrisford**, **A. Bozzo**, **F. Di Guiseppe**, **R.M. Forbes**, **T. Haiden**, **S. Lang**, **M. Mayer**, **I. Polichtchouk**, **I. Sandu**, **F. Vitart** & **N. Wedi**, 2017: Radiation in numerical weather prediction. *ECMWF Technical Memorandum* **No. 816**.

Hogan, **R.J.**, **T. Quaife** & **R. Braghiere**, 2018: Fast matrix treatment of 3D radiative transfer in vegetation canopies: SPARTACUS-Vegetation 1.0. *Geosci. Model Dev.*, **11**, 339–350.

doi:10.21957/sp619ds74g

CERA-SAT: A coupled satellite-era reanalysis

DINAND SCHEPERS, ERIC DE BOISSÉSON, REIMA ERESMAA, CRISTINA LUPU, PATRICIA DE ROSNAY

ECMWF has completed the production of a new research reanalysis, CERA-SAT, which reconstructs the state of the atmosphere, the ocean, sea ice, ocean waves and the land surface between 2008 and 2016. Reanalyses are produced by combining models with observations in a process called data assimilation. The same technique is also used in numerical weather prediction (NWP) to establish the initial conditions on which forecasts are based.

CERA-SAT demonstrates the application of coupled data assimilation in the satellite era. In this context, coupling means that atmospheric, ocean, sea-ice, ocean-wave and land-surface observations are assimilated in a consistent manner. First assessments show that coupling as implemented in CERA-SAT improves the quality of the reanalysis in the tropics but degrades it in the extratropics. The deterioration in the extratropics is believed to be caused by shortcomings in the representation of boundary currents in the coupled model. Insights gained from assessing the performance of CERA-SAT will be used to develop coupled data assimilation in operational weather forecasting and the next generations of ECMWF's reanalyses.

Accounting for coupled processes between Earth system components is beneficial for weather forecasting, a clear example of which is tropical cyclogenesis. For climate assessment purposes, introducing coupling makes it possible to diagnose the key role that the oceans play in storing and transporting heat energy. Heat that is absorbed by the upper ocean eventually affects other components of the Earth system by melting ice shelves, increasing evaporation at the ocean surface, or directly reheating the atmosphere.

Drive towards coupling

The Centre's ten-year Strategy to 2025 places great emphasis on the need to account for all relevant interactions between different components of the Earth system in ECMWF's Integrated Forecasting System (IFS). One aspect of this is the development of a coupled forecasting model accounting for interactions between the atmosphere, the ocean, waves, sea ice and the land surface. Another is the growing research effort being devoted to coupled data assimilation.

A strong push towards increased coupling between Earth system components has been realised in the context of reanalysis production at the Centre. The ECMWF atmosphere-only climate reanalysis capabilities have been extended to include coupling with ocean, sea-ice and land-surface components in the ERA-CLIM2 project.

An important result has been the development of the CERA assimilation system, which enables the simultaneous and coupled assimilation of observations of the atmosphere, ocean, sea-ice and land components of the Earth system (*Laloyaux & Dee*, 2015; *Laloyaux et al.*, 2016). Built around the coupled Earth system model used for ECMWF ensemble (ENS) and seasonal forecasts (SEAS5), the CERA assimilation system makes it possible for ocean observations to have a direct impact on the atmospheric analysis and for atmospheric observations to have an immediate impact on the analysed state of the ocean. The aim is to achieve a consistent analysis of the Earth system. The CERA assimilation system was successfully used to produce CERA-20C (*Laloyaux et al.*, 2017), a 10-member ensemble of coupled climate reanalyses spanning the 20th century while assimilating only a limited range of observation types (surface pressure, marine wind observations and ocean temperature and salinity profiles).

Coupling in CERA-SAT

The CERA-SAT reanalysis applies the CERA data assimilation method to the modern-day observing system, providing a proof of concept for coupled data assimilation with higher model resolutions and the full range of observations used in NWP today.

CERA-SAT combines an eddy-permitting quarter-degree ocean model with an atmosphere modelled at approximately 65 km horizontal resolution (by comparison, CERA-20C has a horizontal resolution of 125 km). The ocean model is constrained by in-situ observations of temperature and salinity profiles and satellite observations of sea-surface height anomalies. For atmospheric assimilation, the full observing system is available, including surface weather stations and satellite observations of temperature, humidity, wind and composition (ozone). At the boundary between the ocean and the atmosphere, ocean waves and sea ice are analysed, the latter using gridded and interpolated sea-ice maps as observations.

Sea-surface temperature is a key driver of the coupling processes between the ocean component and the atmospheric component. In CERA it is relaxed towards an external analysis (OSTIA) during each integration of the coupled model.

The CERA-SAT land data assimilation system is weakly coupled in the sense that it initialises the main land surface prognostic variables of the coupled model: snow water equivalent, snow density, snow temperature, soil temperature and soil moisture, as described by *de Rosnay et al.* (2014). The system uses a combination of conventional observations from the SYNOP network for snow depth, screen level temperature and relative humidity; satellite-based observations of soil moisture from ASCAT on the MetOp series of satellites; and snow cover observations provided by NOAA (US National Oceanic and Atmospheric Administration) from NESDIS (National Environmental Satellite, Data, and

Information Service) IMS (Interactive Multisensor Snow and Ice Mapping System).

The coupling introduced by CERA allows ocean observations to impact the analysed atmospheric state and vice versa through, for instance, heat exchange across the surface of ocean water and sea ice; the interaction of near-surface winds with ocean currents and surface roughness; and the exchange of heat and moisture over land during the 24-hour coupled forecast which provides the background for the analysis.

For more details on the coupling of different Earth system components in CERA-SAT, see Box A and Figure 1.

Coupled data assimilation in CERA-SAT

A

The CERA-SAT reanalysis has been produced using the CERA coupled assimilation system (*Laloyaux et al.*, 2016). This system was set up to use a 24-hour assimilation window shared between the atmospheric, ocean, wave and land components. At the outer-loop level, the atmosphere, land and wave models used in the IFS are coupled in a single executable to the community ocean model NEMO and the LIM2 sea-ice model developed at the Belgian Université catholique de Louvain.

The resulting coupled model is used to produce 24-hour forecasts (the background). The background is combined with observations to produce separate analyses for the atmosphere, ocean, wave, sea-ice and land components. The resulting increments (corrections to the background based on the observations) are then applied in another integration of the coupled model. In effect, this design ensures that interactions between Earth system components are taken into account when observation misfits are calculated as well as when the increments are applied. For CERA-SAT, the CERA system was configured with two such outer-loop iterations.

The CERA-SAT reanalysis additionally includes a separate land surface data assimilation (LDAS) that is weakly coupled by means of a shared coupled model integration using the land surface model H-TESSEL of the IFS (see also Figure 1).

Within the land surface data assimilation, snow cover as well as 2-metre temperature and relative humidity are analysed using a 2-dimensional Optimal Interpolation (OI) scheme. Analysed screen level variables are subsequently used as input for a soil and snow temperature analysis through a 1-dimensional OI scheme, as well as for the soil moisture analysis based on a simplified Extended Kalman Filter (EKF).

Once the second outer loop and the LDAS have been completed, the physically consistent analyses are stored and used to initialise the next analysis cycle.

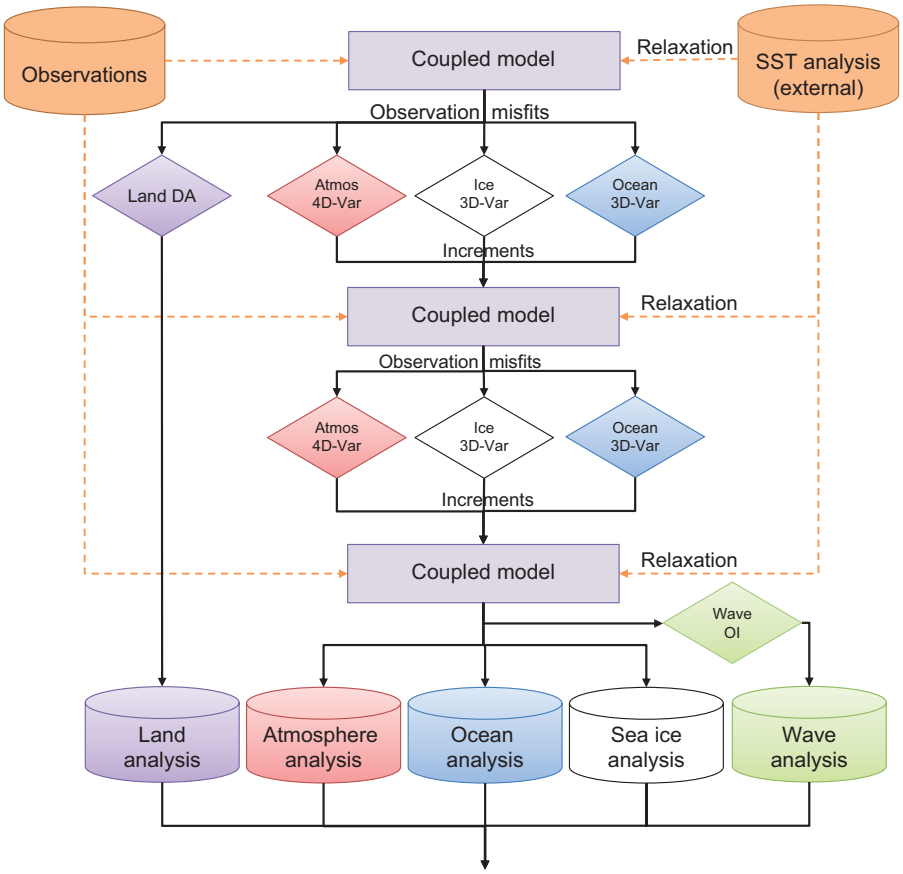

Figure 1 The coupled CERA assimilation system as configured for CERA-SAT production. Observation misfits are derived from the coupled model integration, after which parallel assimilation systems produce analysis increments. These increments are then applied within the coupled model. Repeating this procedure twice in two outer loops makes it possible for the atmosphere, ocean and sea-ice models to reach a balanced state. The land surface analysis (Land DA) is weakly coupled through the first coupled model integration.

doi:10.21957/fd9kz3

The CERA-SAT product

The CERA-SAT reanalysis uses IFS Cycle 42r1 with a horizontal resolution in the atmospheric model of TL319, corresponding to about 65 km, and 137 levels in the vertical reaching up to 0.01 hPa. The ocean component, NEMO v3.4, is specified on the tripolar ORCA025 grid corresponding to an approximate horizontal resolution of 0.25 degrees with a meridional refinement towards the equator. In the vertical, there are 75 levels, with the top level spanning the first metre. The land surface model H-TESSEL comprises four soil layers, including three in the top metre of soil.

In order to produce a reanalysis covering a reasonable number of years within the constraints of available resources, the nine-year CERA-SAT dataset was produced in four separate parts, or production streams. Each stream was initialised with the atmospheric state from the ERA-Interim reanalysis and the ocean state taken from the ORAS5 ocean-only reanalysis. Six months were allowed for spin-up at the start of each stream.

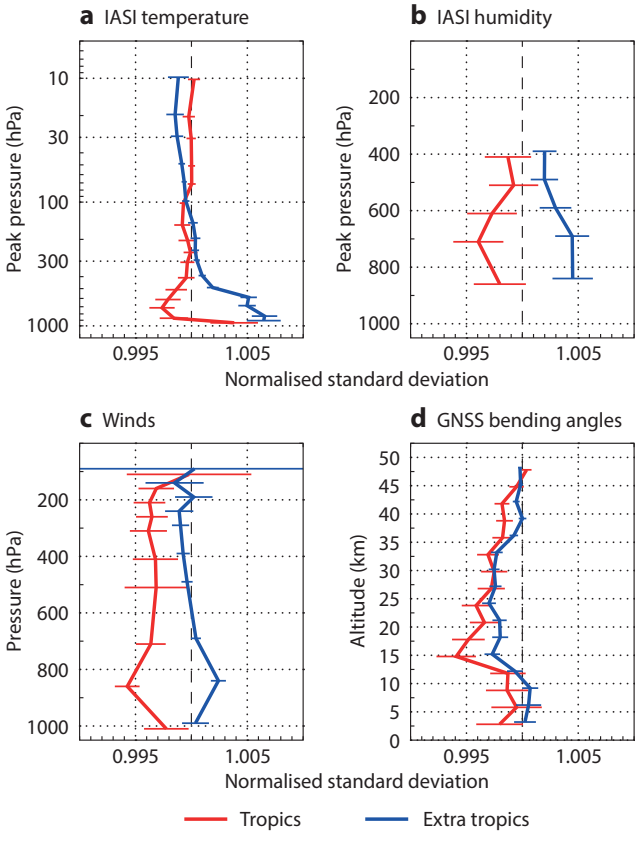

Figure 2 Difference in background departures (CERA-SAT minus CTRL), expressed as the normalised standard deviation, for selected satellite instruments and variables. Values smaller than one indicate a better fit of the background to selected satellite observations in CERA-SAT. The observations are of (a) temperature from the IASI instrument, (b) humidity from the IASI instrument, (c) winds from a suite of instruments and (d) GNSS (Global Navigation Satellite System) bending angles. The comparison spans the full year from September 2015 up to and including August 2016. Bars indicate 95% confidence intervals.

The CERA-SAT reanalysis product is provided as a 10-member ensemble of data assimilations (EDA), each providing analyses of the atmosphere, the ocean, waves, the land surface and sea ice at 3-hourly intervals. In addition to the 137 model levels, the atmospheric product is also made available on 37 pressure levels, 16 potential temperature levels, and the 2 PVU potential vorticity level. The CERA-SAT reanalysis is being made publicly available through ECMWF's Meteorological Archival and Retrieval System (MARS). The atmospheric, land, sea-ice and wave reanalysis can be accessed at *http://apps.ecmwf.int/datasets/*. The data can be selected and retrieved through the MARS Catalogue under the name 'ERA-CLIM2 coupled reanalysis of the satellite era (CERA-SAT)'.

First results

To facilitate impact studies comparing the coupled reanalysis approach used in CERA-SAT with conventional uncoupled reanalysis, a CERA-SAT-like uncoupled control reanalysis (CTRL) was produced in parallel. The control experiment uses the same assimilation setup (window, observing system, etc.) but lacks the interactive ocean and sea-ice components, using a prescribed sea-surface temperature and sea-ice concentration instead and running the uncoupled atmospheric model for both the background and longer-range forecasts.

Improved fit to satellite observations

One way to quantify the impact of the CERA assimilation approach compared to the conventional uncoupled approach is to compare background departures (the difference between observations and a 24-hour forecast, called the background). Generally, smaller background departures signal a (re)analysis that is in better agreement with observations and can thus be said to be of better quality.

The impact of coupled assimilation on background departures is illustrated in Figure 2. It shows the difference in background departures (expressed as normalised standard deviations) between CERA-SAT and CTRL for selected satellite observations averaged over a complete year and stratified for the tropics and the extratropics. From the plots, it is clear that CERA-SAT is consistently closer to observations than CTRL in the tropics, indicating a clear benefit of ocean–atmosphere coupling in that region. The opposite, however, is true in the extratropics, where the coupled reanalysis generally shows a degradation in the background fit to observations.

The degradation in the extratropics is likely a symptom of known shortcomings in the coupled model related to the representation of boundary currents (currents with dynamics that are determined by the presence of a coastline). Through the coupling introduced by CERA, errors in the representation of these currents propagate into the atmospheric analysis, predominantly through an erroneous sea-surface temperature.

These shortcomings are a known feature of the coupled forecast model and are currently accounted for in the

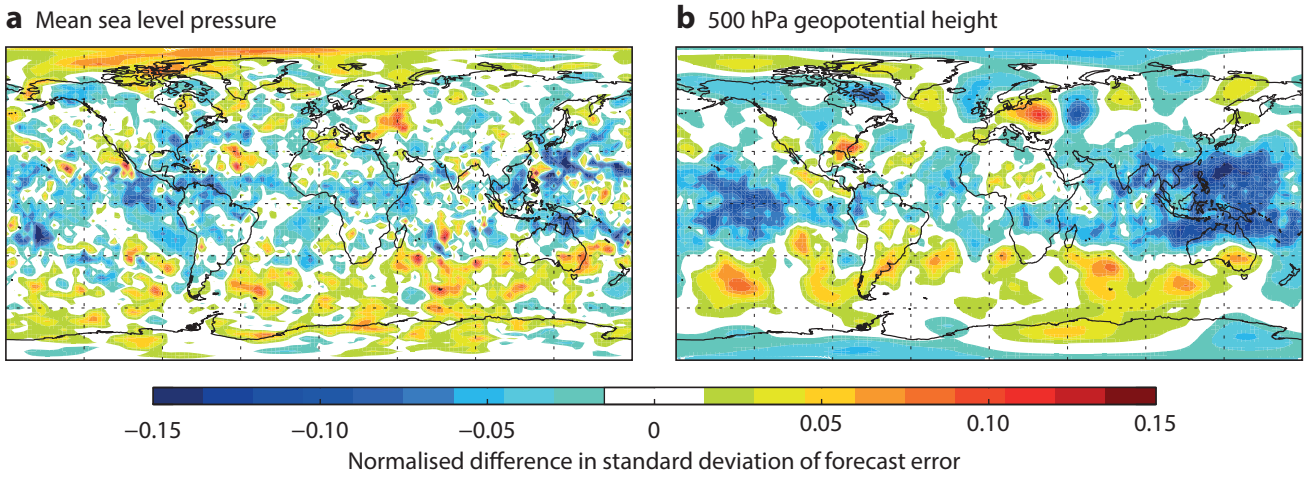

Figure 3 Normalised difference in standard deviation of forecast error for (a) mean sea level pressure and (b) 500 hPa geopotential height, for 5-day forecasts verified against own analysis, between CERA-SAT and CTRL. Blue colours indicate a reduction in standard deviation for CERA-SAT compared to CTRL.

operational ECMWF coupled forecasts by explicitly correcting for them. Work is ongoing to identify the precise cause of these shortcomings and to improve the performance of the coupled model accordingly.

Forecast scores

As an integral part of the CERA-SAT reanalysis production, daily 10-day coupled forecasts were produced, initialised from the 00 UTC coupled analyses. Similarly, uncoupled forecasts (prescribing daily sea-surface temperature and sea-ice concentration valid on the forecast day) were initialised from the uncoupled control reanalysis.

In order to assess the impact of coupling in both the forecast and the data assimilation on forecast performance, forecast error with and without coupling can be compared. Figure 3 shows the difference in the standard deviation of forecast error for 5-day mean sea level pressure and 500 hPa geopotential, verified against own analysis and assessed over a full year, from September 2015 to August 2016. With coupling, reductions in forecast error of up to about 10% are evident in tropical areas, while in the extratropics standard deviations are increased, signalling degraded forecast skill in the CERA-SAT reanalysis with respect to the uncoupled control experiment.

Ocean heat budget

The world's oceans have a tremendous capacity to store heat energy. This stored energy can warm the planet for decades after it is absorbed, hence knowing how much heat energy the ocean absorbs and releases is essential to understand the global climate. The changes in ocean heat content in CERA-SAT have been investigated through an ocean heat budget analysis (Figure 4a). The heat content variation of the total column ocean is equal to the sum of the atmospheric surface heat fluxes, the temperature

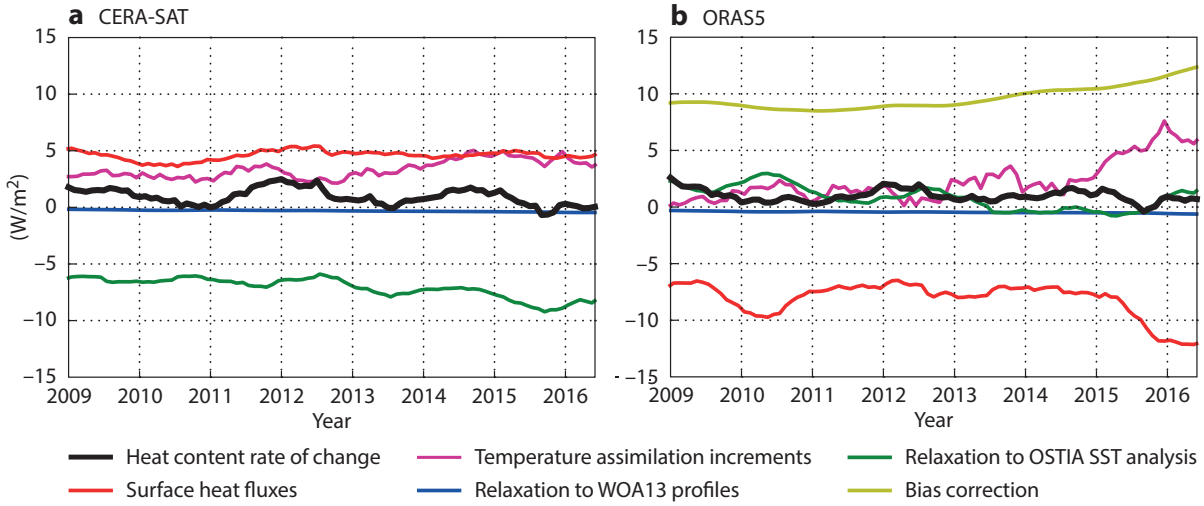

Figure 4 Global ocean heat budget in (a) CERA-SAT and (b) ORAS5. The rate of change in heat content of the total column ocean is the sum of the surface heat fluxes, the temperature assimilation increments, the weak relaxation to the 3-dimensional climatology of temperature/salinity profiles from WOA13 and the relaxation to the OSTIA SST analysis.

assimilation increments, the weak relaxation to the 3-dimensional climatology of temperature and salinity profiles from the World Ocean Atlas 2013 (WOA13), and the relaxation to the OSTIA SST analysis. The 3D relaxation is negligible in well-observed periods. Over the CERA-SAT period, the heat content variations are overall positive indicating a heat gain in the ocean. Both heat fluxes and assimilation increments provide heat to the ocean. The contribution of the SST relaxation to the budget is substantially negative, counteracting the impact of both surface fluxes and increments. The SST relaxation constrains the ocean surface towards the OSTIA SST analysis.

The same kind of ocean heat content analysis has been conducted for the ocean-only reanalysis ORAS5 (Figure 4b). As in CERA-SAT, the ocean gains heat over the whole period, and assimilation increments make a positive contribution to the budget, albeit a relatively small one up to 2014. On the other hand, atmospheric heat fluxes are substantially negative and the SST relaxation is relatively small. The impact of the heat fluxes on the budget is counterbalanced by a bias correction term that was not used in CERA-SAT. This suggests that the bias correction in ORAS5 works to correct the bias resulting from the response to the heat fluxes, similarly to what the SST relaxation does in CERA-SAT. The difference is that the bias correction impacts the whole ocean column while the SST relaxation influences only the top ocean layers. While the total heat content variation is similar in CERA-SAT and ORAS5, the vertical distribution of heat can thus be expected to be different.

This analysis shows that the ocean heat budget is far from resembling a realistic situation, such that variations in ocean heat content result from atmospheric heat fluxes only, and significant research is needed to identify and correct the causes of that. The next CERA system is expected to use a similar ocean bias correction scheme to the one used in ORAS5. Such a scheme has been shown to have a positive impact in the ocean-only analysis system (*Balmaseda et al.*, 2007) and similar behaviour is expected in CERA (*Feng et al.*, 2017).

CERA-SAT in the reanalysis portfolio

The performance of CERA-SAT lies between that of two existing ECMWF reanalyses of the satellite era. Figure 5 shows time series of 500 hPa geopotential height and 2-metre temperature forecast scores over Europe. Here, forecast performance is expressed as the lead time at which the anomaly correlation (against own analysis) drops below a certain threshold: 95, 80 or 60 per cent in this case. In this metric, longer lead times indicate a better reanalysis.

CERA-SAT is compared to two other reanalyses: ERA-Interim and ERA5 (*Hersbach & Dee*, 2016). ERA-Interim is the current operational reanalysis produced at ECMWF, based on a 12-year-old IFS release. It provides an atmospheric reanalysis with approximately 80-kilometre spatial resolution on 60 vertical levels. ERA-Interim is scheduled to be phased out and replaced by ERA5, which is currently being produced at ECMWF for the EU-funded Copernicus Climate Change Service (C3S) operated by the Centre.

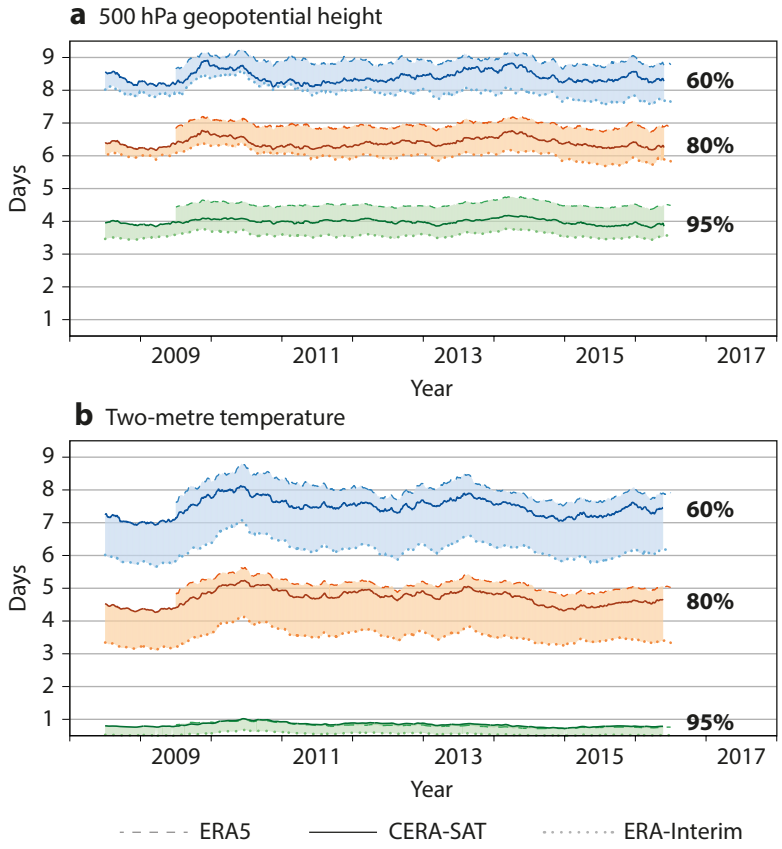

Figure 5 Time evolution of forecast skill in Europe for (a) 500 hPa geopotential height and (b) 2-metre temperature forecasts produced using ERA-Interim, ERA5 and CERA-SAT, expressed in terms of the number of days after which the anomaly correlation coefficient (12-month running mean) falls below a certain threshold (60, 80 and 95%).

ERA5 benefits from a recent IFS cycle (41r2) and provides atmospheric fields at about 30 km resolution on 137 levels. ERA5 is currently publicly available from 2010 onward.

Clearly, CERA-SAT is not able to match the overall quality of ERA5, while comfortably beating the ageing ERA-Interim reanalysis. The deficit with respect to ERA5 is likely related to the higher model resolution of ERA5 as well as the aforementioned shortcomings in boundary current representation in the coupled model propagating into the atmospheric reanalysis in the CERA system.

The CERA-SAT reanalysis has been produced first and foremost as an experimental dataset to aid research and development work undertaken at ECMWF towards coupled data assimilation and climate reanalysis. As such, it cannot be expected to perform as well as the current generation of ECMWF reanalysis products in terms of quality, temporal coverage and user support.

Outlook

CERA-SAT can serve as a proof of concept for using the CERA system in the context of the modern-day NWP observing system. As a result, efforts are now under way at ECMWF to implement and evaluate a version of CERA in the operational codebase and to correct the problems with boundary current representation in the coupled model. CERA-SAT will thus facilitate the future implementation of coupled data assimilation in operational weather forecasting and in the next generation of ECMWF reanalyses. The former holds the promise of more consistent Earth system analyses and, as a result, better forecasts. The latter will help us to better understand the changing climate and to assess and predict its impact.

FURTHER READING

Balmaseda, **M. A.**, **D. Dee**, **A. Vidard**, **D. L. T. Anderson**, 2007: A multivariate treatment of bias for sequential data assimilation: Application to the tropical oceans. *Q. J. R. Meteorol. Soc.*, **133**, 167–179.

Feng, **X.**, **K. Haines**, **E. de Boisseson**, 2017: Assessment of coupled-model drift and approaches for obtaining consistent ocean and atmosphere bias corrections. *ERA-CLIM2 project. Deliverable 2.10.* (*www.era-clim2.eu/products*)

Hersbach, **H.** & **D. Dee**, 2016: ERA5 reanalysis is in production. *ECMWF Newsletter* **No. 147**, 7.

Laloyaux, **P.** & **D. Dee**, 2015: CERA: A coupled data assimilation system for climate reanalysis. *ECMWF Newsletter* **No. 144**, 15–20.

Laloyaux, **P.**, **M. Balmaseda**, **D. Dee**, **K. Mogensen** & **P. Janssen**, 2016: A coupled data assimilation system for climate reanalysis. *Q. J. R. Meteorol. Soc.*, **142**, 65–78.

Laloyaux, **P.**, **E. de Boisséson** & **P. Dahlgren**, 2017: CERA-20C: An Earth system approach to climate reanalysis. *ECMWF Newsletter* **No. 150**, 25–30.

de Rosnay P., **G. Balsamo**, **C. Albergel**, **J. Muñoz-Sabater** & **L. Isaksen**, 2014: Initialisation of land surface variables for Numerical Weather Prediction, *Surveys in Geophysics*, **35(3)**, 607–621.

ECMWF Calendar 2018

Apr 23–27	NWP training course: Physical parametrization of sub-grid scale processes
Apr 24	Policy Advisory Committee
Apr 25–26	Finance Committee
Apr 30 – May 4	NWP training course: Predictability and ensemble forecast systems
May 8–9	Workshop on hydrological services for business
May 15–16	Security Representatives' meeting
May 16–18	Computing Representatives' meeting
May 21–24	Workshop on radiation in the next generation of weather forecast models
Jun 4	Workshop on Early Warning Centres
Jun 5–8	Using ECMWF's Forecasts (UEF)
Jun 9–10	Hackathon 2018
Jun 13–14	Council
Jul 10–12	Workshop on physics–dynamics coupling (PDC18)
Sep 10–13	Annual Seminar
Sep 24–28	Workshop on high-performance computing in meteorology
Oct 1–3	Training course: Use and interpretation of ECMWF products
Oct 8–10	Scientific Advisory Committee
Oct 11–12	Technical Advisory Committee
Oct 22–23	Finance Committee
Oct 24	Policy Advisory Committee
Dec 4–5	Council
Apr 2–5 2019	Workshop on predictability, dynamics and applications research using the TIGGE and S2S ensembles

ECMWF publications

(see *http://www.ecmwf.int/en/research/publications*)

Technical Memoranda

820 **Dahlgren**, **P.**: Evaluation and diagnostics of the CERA-20C climate reanalysis ensemble. *January 2018*

818 **Richardson**, **D.S.**, **T. Hewson**: Use and verification of ECMWF products in Member and Co-operating States. *January 2018*

813 **Janssen**, **P.A.E.M.**: Shallow-water version of the freak wave warning system. *November 2017*

EUMETSAT/ECMWF Fellowship Programme Research Reports

46 **Lean**, **K.**, **N. Bormann**: Indian Ocean AMVs: Moving to Meteosat-8 and assessing alternative options. *January 2018*

ESA Contract Reports

Rennie, **M.**: CCN6 results: further Chain-of-Processors testing of L2B results and of the CCN6 L2B processor algorithm updates. *October 2017*

Rennie, **M.**, **de Kloe**, **J.**: Assessment of Level-2B wind errors resulting from realistic simulation of ISR/IRC/AUX_RBC calibration chain. *January 2017*

Contact information

ECMWF, Shinfield Park, Reading, Berkshire RG2 9AX, UK

Telephone National 0118 949 9000

Telephone International +44 118 949 9000

Fax +44 118 986 9450

ECMWF's public website http://www.ecmwf.int/

E-mail: The e-mail address of an individual at the Centre is firstinitial.lastname@ecmwf.int. For double-barrelled names use a hyphen (e.g. j-n.name-name@ecmwf.int).

For any query, issue or feedback, please contact ECMWF's Service Desk at *servicedesk@ecmwf.int*.

Please specify whether your query is related to forecast products, computing and archiving services, the installation of a software package, access to ECMWF data, or any other issue. The more precise you are, the more quickly we will be able to deal with your query.

Index of Newsletter articles

This is a selection of articles published in the *ECMWF Newsletter* series during recent years.
Articles are arranged in date order within each subject category.
Articles can be accessed on ECMWF's public website – http://www.ecmwf.int/en/research/publications

ECMWF
Newsletter | Number 155 – Spring 2018
European Centre for Medium-Range Weather Forecasts
www.ecmwf.int